General Disclaimer

One or more of the Following Statements may affect this Document

- This document has been reproduced from the best copy furnished by the organizational source. It is being released in the interest of making available as much information as possible.

- This document may contain data, which exceeds the sheet parameters. It was furnished in this condition by the organizational source and is the best copy available.

- This document may contain tone-on-tone or color graphs, charts and/or pictures, which have been reproduced in black and white.

- This document is paginated as submitted by the original source.

- Portions of this document are not fully legible due to the historical nature of some of the material. However, it is the best reproduction available from the original submission.

TWO-ELECTRON BOND-ORBITAL MODEL II.

Chuping Huang*, John A. Moriarty†, and A. Sher*

Department of Physics

College of William and Mary

Williamsburg, Virginia 23185

* Supported in part by Grant No. NSF-DMR75-02365

† Supported in part by Grant No. NASA-NSG-1089

ABSTRACT

The two-electron bond-orbital model of tetrahedrally-coordinated solids is generalized and its application extended. All intrabond matrix elements entering the formalism are now explicitly retained, including the direct overlap S between the anion and cation sp^3 hybrid wavefunctions. Complete analytic results are obtained for the six two-electron eigenvalues and eigenstates of the anion-cation bond in terms of S, one-electron parameters V_2 and V_3, and two-electron correlation parameters V_4, V_5 and V_6. Refined formulas for the dielectric constant and the nuclear exchange and pseudodipolar coefficients, as well as new expressions for the valence electron density, polarity of the bond and the cohesive energy, are then derived. A scheme for evaluating the basic parameters of the model is established, in which V_2 is fit to the optical-absorption peak of group-IV elements in the manner of Harrison and Ciraci and the remaining quantities are calculated using Hartree-Fock free-atom wavefunctions and term values. For the twenty group-IV and III-V semiconductors, we find $V_5 \sim V_6 \sim 0$ but $V_4/V_2 \sim 1/2$, leading to significant correlation effects in most properties. The theory gives a good account of the experimentally observed trends in all properties considered and approximate quantitative agreement is achieved for the pseudodipolar coefficient. Good agreement is also obtained for the E_2 optical-absorption peak, the dielectric constant, the nuclear exchange coefficient and the cohesive energy of the binary compounds by scaling to experiment for the group-IV elements. Our calculations on the cohesive energy suggest that the intrabond overlap energy,

discarded by Harrison and Ciraci, is an essential source of positive cohesion and probably rules out any major role by the interbond van der Waals interaction suggested by them. The valence electron density is found to be dominated by the polarity and the shape of the sp^3 hybrids. The preliminary indication is that the long-range tails of the free-atom s and p wavefunctions must be contracted to account for the observed bond density in Si.

I. INTRODUCTION

The description of the valence bands of tetrahedrally-coordinated solids in terms of sp^3 hybrid wavefunctions has been considered at various times by a number of different workers. In recent papers, Harrison[1] and Harrison and Ciraci[2] (hereafter referred to as HC) have presented a unified and greatly extended version of such a theory, which they call the bond-orbital model. One of the major contributions of their work was the direct treatment of a wide range of physical properties in addition to the band structure. In this model the band structure becomes a separate question[3] and a large number of properties can be calculated with only a knowledge of the local properties of the anion-cation bond. Formally, this bond is equivalent to a two-electron diatomic molecule. Harrison[1] and HC, as well as previous solid-state workers, have treated this molecule in the usual one-electron, molecular-orbital approximation. As a step toward providing a more complete treatment of the bond, we introduced in the first paper[4] of this series (hereafter referred to as Paper I) a direct two-electron formalism. Our two-electron bond-orbital model was developed as an extension of the method of Falicov and Harris[5] for treating the hydrogen molecule. In Paper I we considered the simplest special cases of the theory and applied the results to the calculation of the dielectric constant and the nuclear exchange and pseudodipolar coefficients. In this paper we generalize our two-electron bond-orbital model into a full quantitative theory and extend its application to several additional physical properties, attempting to assess the importance of two-electron correlation in each case.

The simplicity of any bond-orbital approach rests with three approximations. First, the appropriate anion and cation sp^3 hybrids are assumed to form a complete set for the description of the bond. If the s and p wavefunctions making up these hybrids are atomic-like states, this set is technically undercomplete, although the choice of states can be optimized. In a one-electron description, one then has a simple two-state eigenvalue problem and the ground-state or bond orbital is a symmetric linear combination of two sp^3 hybrids. In a two-electron description, a six-state eingenvalue problem must be solved, but an exact analytic solution is still possible for the two-electron bond-orbital, as well as all of the excited states. In either case, the bond orbitals obtained are then assumed to be orthogonal to one another in the solid. This is approximately true because the four sp^3 hybrids sharing a common atomic site are orthogonal by construction.[1] Finally, all matrix elements linking the ground state of one bond to the excited states of its neighbors are discarded. The only interbond matrix elements permitted, and the ones which give rise to the band structure,[2,3] are those connecting neighboring bond orbitals through the Hamiltonian. Then, because the valence band is full, one can make a unitary transformation from extended Block states to the localized bond-orbitals in calculating both the total energy and the total valence-electron density of the solid. These latter quantities are thus given, respectively, as just a sum of the total energies and a sum of the total electron densities of the individual bonds and are exactly independent of the remaining interbond terms. Thus physical properties which depend only on the total energy or electron density can be calculated entirely in terms of intrabond matrix elements.

The work begun in Paper I is extended here in several major ways. We first obtain a complete solution of the two-electron problem. The direct overlap

matrix element between anion and cation hybrids and the two-center Coulomb exchange and transfer integrals, all of which were dropped in Paper I, are now included without approximation. In Sec. II exact analytic results for the singlet and triplet eigenstates and eigenvalues are obtained. We then proceed to develop a full formal theory of several important physical properties. In addition to a refined treatment of the dielectric constant and indirect nuclear interactions, we consider the valence electron density, the polarity of the bond and the cohesive energy. In Sec. III a procedure for quantitatively evaluating the basic parameters of the theory is established and application of the formal results of Sec. II is made to twenty tetrahedrally-bonded solids.

II. FULL THEORY INCLUDING OVERLAP

A. Eigenvalues and Eigenstates

When the overlap between anion and cation hydrids is retained, the second-quantization formalism employed in Paper I loses its simplicity and elegance. Thus in this paper we introduce a spacial representation. As in Paper I, it is possible here to proceed with a basis set of the six two-electron states $|a\uparrow a\downarrow\rangle$, $|c\uparrow c\downarrow\rangle$, $|a\uparrow c\uparrow\rangle$, $|a\downarrow c\downarrow\rangle$, $|a\uparrow c\downarrow\rangle$, and $|c\uparrow a\downarrow\rangle$. However, both of the physics and the mathematics are simplified if a basis set of three singlet and three triplet states is chosen from the outset. Then the six-by-six Hamiltonian matrix block diagonalizes into two three-by-three blocks. One of these two blocks, that associated with the triplets, is also diagonal with all three diagonal elements equal.

We begin by defining three orthonormal triplet states in the coordinate representation:

$$|1\rangle = \frac{1}{\sqrt{1-S^2}}|a\uparrow c\uparrow\rangle = \Phi_A(\vec{r}_1,\vec{r}_2)\sigma_\uparrow(1)\sigma_\uparrow(2)$$

$$|2\rangle = \frac{1}{\sqrt{1-S^2}}|a\downarrow c\downarrow\rangle = \Phi_A(\vec{r}_1,\vec{r}_2)\sigma_\downarrow(1)\sigma_\downarrow(2) \qquad (1)$$

$$|3\rangle = \frac{1}{\sqrt{1-S^2}}\left(|a\uparrow c\downarrow\rangle - |c\uparrow a\downarrow\rangle\right) = \frac{1}{\sqrt{2}}\Phi_A(\vec{r}_1,\vec{r}_2)\left[\sigma_\uparrow(1)\sigma_\downarrow(2) + \sigma_\uparrow(2)\sigma_\downarrow(1)\right]$$

where $\Phi_A(\vec{r}_1, \vec{r}_2)$ is the anti-symmetric spatial function

$$\Phi_A(\vec{r}_1, \vec{r}_2) = \frac{1}{\sqrt{2(1-S^2)}} \left[\phi_a(\vec{r}_1)\phi_c(\vec{r}_2) - \phi_c(\vec{r}_1)\phi_a(\vec{r}_2) \right] . \tag{2}$$

In Eqs. (1) and (2) $\phi_a(\vec{r})$ and $\phi_c(\vec{r})$ are respectively the anion and cation hybrid wavefunctions, S is the overlap integral between them:

$$S = \int \phi_a^*(\vec{r})\,\phi_c(\vec{r})\,d\vec{r} , \tag{3}$$

and $\sigma_\uparrow$ and $\sigma_\downarrow$ are the usual one-electron spin functions. We next define three normalized singlet states:

$$\begin{aligned} |4\rangle &= |a\uparrow a\downarrow\rangle = \phi_a(\vec{r}_1)\,\phi_a(\vec{r}_2)\,\Sigma_A \\ |5\rangle &= |c\uparrow c\downarrow\rangle = \phi_c(\vec{r}_1)\,\phi_c(\vec{r}_2)\,\Sigma_A \\ |6\rangle &= \frac{1}{\sqrt{2(1+S^2)}} \left(|a\uparrow c\downarrow\rangle + |c\uparrow a\downarrow\rangle \right) = \frac{1}{\sqrt{2(1+S^2)}} \left[\phi_a(\vec{r}_1)\phi_c(\vec{r}_2) + \phi_c(\vec{r}_1)\phi_a(\vec{r}_2) \right] \Sigma_A \end{aligned} \tag{4}$$

where Σ_A is the anti-symmetric spin function

$$\Sigma_A = \frac{1}{\sqrt{2}} \left[\sigma_\uparrow(1)\,\sigma_\downarrow(2) - \sigma_\uparrow(2)\,\sigma_\downarrow(1) \right] . \tag{5}$$

The singlets are automatically orthogonal to the triplets because of the orthonormality of $\sigma_\uparrow$ and $\sigma_\downarrow$, but the singlets are not mutually orthogonal to one another:

$$\begin{aligned} \langle 4|5\rangle &= S^2 \\ \langle 4|6\rangle &= \langle 5|6\rangle = S\left(\frac{2}{1+S^2}\right)^{\frac{1}{2}} \end{aligned} \tag{6}$$

The two-electron Hamiltonian operator has the form

$$H(\vec{r}_1, \vec{r}_2) = H_0(\vec{r}_1) + H_0(\vec{r}_2) + \frac{e^2}{|\vec{r}_1 - \vec{r}_2|} , \tag{7}$$

where H_0 is the sum of a kinetic energy operator T and an external potential V_{ext}:

$$H_0(\vec{r}) = T(\vec{r}) + V_{ext}(\vec{r}) . \tag{8}$$

The quantity V_{ext} includes bare-ion potentials from the anion and the cation plus the potential associated with all other bonds in the crystal. Because the full Hamiltonian H has no spin-operator dependence, all matrix elements coupling singlet and triplet states vanish, and the secular determinant has the simple block structure

$$\begin{vmatrix} E_T - E & 0 \\ 0 & \langle i|H|j\rangle - \langle i|j\rangle E \\ & i,j = 4,5,6 \end{vmatrix} = 0 , \tag{9}$$

where $E_T = \langle 1|H|1\rangle = \langle \Phi_A|H|\Phi_A\rangle$. We may write out the matrix elements entering Eq. (9) explicitly in terms of familiar one- and two-center integrals. Following HC and Paper I, we define[6] the one-electron expectation values

$$\varepsilon_{nc} = \int \phi_n^*(\vec{r})\, H_c(\vec{r})\, \phi_n(\vec{r})\, d\vec{r} , \qquad n = a, c , \tag{10}$$

and the (positive) transfer or hopping integral

$$V_{2n} = -\int \phi_n(\vec{r}) H_{\text{ion}}(\vec{r}) \phi_c(\vec{r})\, d\vec{r} \quad . \tag{11}$$

All of the two-center Coulomb integrals have the form

$$I(n,n' \mid m,m') = \int \phi_n^*(\vec{r}_1)\, \phi_{n'}^*(\vec{r}_2)\, \frac{e^2}{|\vec{r}_1 - \vec{r}_2|}\, \phi_m(\vec{r}_1)\, \phi_{m'}(\vec{r}_2)\, d\vec{r}_1\, d\vec{r}_2 \quad , \tag{12}$$

$$n, n', m, m' = a, c \quad .$$

The Coulomb replusive energy of two electrons on the same ion site is

$$U_n = I(n,n \mid n,n), \qquad n = a, c \quad , \tag{13}$$

while the corresponding energy with one electron on each site is

$$K = I(a,c \mid a,c). \tag{14}$$

The exchange energy is

$$J = I(a,c \mid c,a) \quad , \tag{15}$$

and finally the transfer energy (analogous to V_{2n}) is

$$H_n = I(n,n \mid a,c), \qquad n = a, c \quad . \tag{16}$$

In Paper I we neglected, in addition to the overlap matrix element S, the quantities J and H_n. It is easily seen from Eq. (12) that J and H_n, unlike U_n and K, will vanish as $S \to 0$, so that the theory of Paper I becomes rigorous in that limit. In the real semiconductors of interest, of course, the overlap is large, $S \sim 0.6$, and J and H_n will have magnitudes comparable to U_n and K. Our calculations, which are discussed in Sec. III, show that for homopolar solids like the group-IV elements

$$U_n > K > H_n > J \tag{17}$$

with $J \sim \frac{1}{2} U_n$. Similar trends exist for the binary compounds, where in addition

$$U_a > U_c \qquad \text{and} \qquad H_a > H_c \tag{18}$$

because the anion hybrid is usually less spatially extended than the cation hybrid. In our calculations Eq. (18) holds for all III-V compounds except BP and BAs where the inequalities are reversed, as discussed in Sec. III.

In order to simplify the analysis and to make contact with HC and Paper I, it is also useful to define the following combinations of the above quantities:

$$\begin{aligned}
\varepsilon_n &\equiv \varepsilon_{n0} + K \,, \qquad n = a, c \\
V_2^c &\equiv V_{20} - \tfrac{1}{2}(H_a + H_c) + \tfrac{1}{2} S(\varepsilon_a + \varepsilon_c) \\
V_3^c &\equiv \tfrac{1}{2}\left[(\varepsilon_c - \varepsilon_a) - \tfrac{1}{2}(U_a - U_c)\right] \\
V_4^c &\equiv \tfrac{1}{2}\left[\tfrac{1}{2}(U_a - U_c) - K\right] \\
V_5^c &\equiv \tfrac{1}{2}\left[\tfrac{1}{2} S(U_a - U_c) - (H_a - H_c)\right]
\end{aligned} \tag{19}$$

$V_t' = \Sigma (H_a + H_c) - J - S^2 K$

Because of the overall charge neutrality of the solid, its energy levels will only depend on absolute differences of the one- and two-center Coulomb integrals defined in Eqs. (10) - (16). The energies defined in Eq. (19) correctly reflect this fact. For example, the addition of K to ε_{a0} has the effect of screening the bare-ion potential arising from the cation and gives ε_a a magnitude close to a Hartree-Fock expectation value, as shown by Eq. (28) of Paper I. Then $\frac{1}{2}(\varepsilon_a + \varepsilon_c)$ is the center of gravity of the one-electron band structure and the term $\frac{1}{2} S (\varepsilon_a + \varepsilon_c)$ removes exactly the dependence of V_{20} on the zero of energy. The energies V_2° and V_3' are conceptually similar to the one-electron HC parameters which we denote as V_2^{HC} and V_3^{HC}. The quantities $\frac{1}{2}(H_a + H_c)$ and $\frac{1}{2}(U_a - U_c)$ are appropriate average values of the electron-electron interaction, which physically screens V_{ext} and reduces the magnitudes of V_2° and V_3°. More specifically, V_2 and V_3° are derivable from the one-electron Hamiltonian

$$H_{one}(\vec{r}) = H_0(\vec{r}) + \int \frac{[\phi_a^*(\vec{r}')\phi_a(\vec{r}') + \phi_c^*(\vec{r}')\phi_c(\vec{r}')]\, d\vec{r}'}{|\vec{r} - \vec{r}'|} - \frac{1}{2}(\varepsilon_a + \varepsilon_c) \tag{20}$$

by the tight-binding formulas

$$V_2^\circ = -\langle \phi_a | H_{one} | \phi_c \rangle$$
$$V_3^\circ = \frac{1}{2}\left[\langle \phi_c | H_{one} | \phi_c \rangle - \langle \phi_a | H_{one} | \phi_a \rangle\right] \tag{21}$$

We emphasize, however, that V_2^0 and V_3^c enter the present theory only as definitions. All two-electron correlation corrections to the screening are included exactly through the remaining parameters V_1^c, V_4^c and V_6^c. The quantity V_1^c is a simple generalization of the correlation term defined in Eq. (21a) of Paper I, while V_5^c and V_6^c appear as a result of the finite values of S, J and H_n. Interestingly, even for large values of S our calculated values of V_5^0 and V_6^0 always turn out to be negligible and the dominant correlation parameter is V_4^0, as we assumed in Paper I. Finally, we should point out the symmetry properties of our new quantities. The energies V_2^c, V_4^0 and V_6^c involve symmetric combinations of ε_n, U_n, and H_n, as well as the symmetric quantities V_{20}, S, K and J. Consequently, V_2^0, V_4^c and V_6^c are covalent energies which depend primarily on bond length and not on the polarity of the bond. The energies V_3^c and V_5^0, on the other hand, are antisymmetric in ε_n, U_n and H_n and thus vanish identically for homopolar solids. We may already anticipate that for negligible V_5^c and V_6^c the effect of two-electron correlation will be to increase the covalency and decrease the polarity of the bond in binary compounds, because $V_4^0 > 0$.

The eigenvalue E_T of Eq. (9) associated with the degenerate triplet states can be evaluated immediately:

$$E_M = E_T = \varepsilon_a + \varepsilon_c - K + (2S V_2^0 + V_6^c)/(1-S^2), \quad M = I, II, III. \tag{22}$$

The eigenvalues associated with the three singlet states may be written as

$$E_M = \varepsilon_a + \varepsilon_c - K + E_M^0, \quad M = IV, V, VI, \tag{23}$$

where E_M^0 is a solution of the determinantal equation

$$\begin{vmatrix} -2V_1^{\circ} - V^{\circ} - E_M^{\circ} & 2SV_4^{\circ} - V_6^{\circ} - S^2E_M^{\circ} & -V_5^{\circ} - SV_3^{\circ} - V_6^{\circ} - SE_M^{\circ} \\ 2SV_4^{\circ} - V_6^{\circ} - SE_M^{\circ} & 2V_4^{\circ} + 2V_3^{\circ} - E_M^{\circ} & -V_5^{\circ} - SV_3^{\circ} + V_6^{\circ} - SE_M^{\circ} \\ -V_5^{\circ} - SV_3^{\circ} - V_6^{\circ} - SE_M^{\circ} & -V_5^{\circ} + SV_3^{\circ} + V_6^{\circ} - SE_M^{\circ} & \frac{1}{2}[-2SV_2^{\circ} - V_4^{\circ} - (1+S^2)E_M^{\circ}] \end{vmatrix} = 0 \qquad (24)$$

Equation (24) is, of course, just a cubic equation in E_M° and reduces to Eq. (20) of Paper I in the limit $S = V_5^{\circ} = V_6^{\circ} = 0$. As in Paper I, the physical content of the solutions of Eq. (24) is most transparent in the two special cases where this equation factorizes. These cases are: (1) $V_3^{\circ} = V_5^{\circ} = 0$, which is the appropriate solution for the group-IV elements, and (2) $V_4^{\circ} = V_5^{\circ} = V_6^{\circ} = 0$, which is the limit of no two-electron correlation. Following Paper I, we denote the former case as the Falicov-Harris limit (hereafter referred to as the FH limit) and the latter as the Harrison limit.

In the FH limit the energy eigenvalues and the splittings between them may be expressed as

$$\begin{aligned} E_{I,II,III} &= 2\varepsilon - K + 2SV_2 + V_6 - 2S^2(V_4 - V_6)/(1-S^2) \\ E_{IV} &= 2\varepsilon - K + 2SV_2 + 2V_4 + V_6 - 2S^2(V_4 - V_6)/(1-S^2) \\ E_{V,VI} &= 2\varepsilon - K + 2SV_2 + V_4 - V_6 \pm (4V_2^2 + V_4^2)^{\frac{1}{2}} \end{aligned} \qquad (25)$$

and

$$\begin{aligned} E_{IV} - E_{VI} &= 2V_6/(1-S^2) + V_4(1-3S^2)/(1-S^2) + (4V_2^2 + V_4^2) \\ E_{III} - E_{I} &= 2V_4 \\ E_{I} - E_{III} &= 2V_6/(1-S^2) - V_4(1+S^2)/(1-S^2) + (4V_2^2 + V_4^2) \end{aligned} \qquad (26)$$

where we have dropped the subscripts a and c on $\mathcal{E}$ and have introduced the renormalized variables

$$
\begin{aligned}
V_2 &= [\,V_2' + S(V_4 - V_5)\,]/(1-S^2) \\
V_3 &= V_3'/(1-S^2)^{\frac{1}{2}} \\
V_4 &= V_4'/(1-S^2) \\
V_5 &= V_5'/(1-S^2) \\
V_6 &= V_6'/(1-S^2)
\end{aligned}
\tag{27}
$$

which facilitate comparisons with HC and Paper I and which will be used in the remainder of this paper. The renormalization factors of $(1-S^2)^{1/2}$ and $(1-S^2)$ are precisely the same as those used by HC in defining V_3^{HC} and V_2^{HC}, respectively. The term added to V_2^c may be viewed as the subtraction of the constant $V_4 - V_6$ from H_{one} in Eq. (20). The qualitative ordering of the energy levels in Eq. (25) is the same as given in Fig. 1 of Paper I, with E_{VI} the ground state energy and the triplet levels and the first excited singlet E_{IV} separated by $2V_4$. Note that overlap has shifted all six levels upward in energy by an amount $2SV_2$. This term, however, will contribute only to properties which depend on the absolute position of the levels, such as the cohesive energy. For $V_6 = 0$ the triplet energies and E_{IV} are also shifted downward from the center of gravity by $2S^2V_4/(1-S^2)$. This means that if one fits $E_{IV} - E_{VI}$ to the principal optical absorption gap for a fixed V_4, as we did in Paper I and as we do in Sec. III below, one requires a larger value of V_2 than with $S = 0$.

In the Harrison limit the energy levels and splittings are found to be

$$
\begin{aligned}
E_{I,II,III} &= E_{IV} = \mathcal{E}_a + \mathcal{E}_c - K + 2SV_2 \\
E_{V,VI} &= \mathcal{E}_a + \mathcal{E}_c - K + 2SV_2 \pm 2(V_2^2 + V_3^2)^{\frac{1}{2}}
\end{aligned}
\tag{28}
$$

and

$$E_{IV} - E_{V} \quad E_{I} - E_{II} = 2\left(V_2^2 + V_3^2\right)^{\frac{1}{2}}$$
$$E_{I} - E_{IV} = 0 \tag{29}$$

Again all levels are shifted by the amount $2S\mathrm{V}_2$ which is consistent with the shift of $S\mathrm{V}_2$ in the one-electron energy levels of HC. Otherwise, overlap has not altered the formal structure of the eigenvalues and Eqs. (28) and (29) are completely equivalent to the HC results, as discussed in Paper I.

We next consider the calculation of the eigenfunction of the Hamiltonian H. It is evident from Eq. (9) that the three triplet basis states are already eigenstates of H:

$$|\mathrm{I}\rangle = |1\rangle$$
$$|\mathrm{II}\rangle = |2\rangle \tag{30}$$
$$|\mathrm{III}\rangle = |3\rangle$$

The singlet eigenstates can be written as a linear combination of the three singlet basis states:

$$|M\rangle = \sum_{i=4,5,6} a_{iM}\,|i\rangle \quad , \qquad M = \mathrm{IV}, \mathrm{V}, \mathrm{VI} \quad . \tag{31}$$

The ground state $|\mathrm{VI}\rangle$ is the two-electron bond orbital. Setting

$$a_{iM} = A_{iM} / D \quad , \tag{32}$$

where D is the normalization constant

$$D = \left[A_{4M}^2 + A_{5M}^2 + A_{6M}^2 + 2S^2 A_{4M} A_{5M} + 2S\sqrt{1+S^2}\,(A_{4M} + A_{5M}) A_{6M} \right]^{-\frac{1}{2}}, \tag{33}$$

the coefficients A_{iM} are obtained in the usual way and may be expressed as

$$\begin{Bmatrix} A_{4M} \\ A_{5M} \end{Bmatrix} = \frac{1}{\sqrt{1+S^2}} \Big\{ \left[(-2SV_2 - V_6)(1-S^2) + 2S(V_4 - V_6) - S^2 E_M^0 \right] \left[-V_2(1-S^2) \right.$$
$$+ S(V_4 - V_6) \pm (SV_3 + V_5)(1-S^2)^{\frac{1}{2}} - S E_M^0 \Big] - \left[2V_4(1-S^2) \pm 2V_3(1-S^2)^{\frac{1}{2}} \right.$$
$$\left. - E_M^0 \right] \left[-V_2(1-S^2) + S(V_4 - V_6) \mp (SV_3 + V_5)(1-S^2)^{\frac{1}{2}} - S E_M^0 \right] \Big\} \tag{34}$$

$$A_{6M} \quad \left[-2V_1(1-S^2) - E_M^0 \right]^2 - 4V_3^2(1-S^2) - \left[(2SV_2 - V_6)(1-S^2) \right.$$
$$\left. + 2S^2(V_4 - V_6) - S^2 E_M^0 \right] .$$

In the general case, once the roots of the cubic equation (9) are found, they can be inserted into Eq. (34) to find the A_{iM}.

In the FH limit, $A_{iM} = D = 0$ for $M = IV$ and the general solution Eq. (34) cannot be used. In this case, the proper coefficients can be shown to be

$$\begin{Bmatrix} a_{4\,IV} \\ a_{5\,IV} \end{Bmatrix} = \pm 1/\sqrt{2(1+S^2)} \tag{35}$$

$$a_{6\,IV} = 0$$

For $M = V, VI$, on the other hand, Eq. (25) may be used directly in Eq. (34) to obtain

$$a_{4M} = a_{5M} = 4\left[2(1+S^2) \pm SQ\right]/D_0$$
$$a_{6M} = 4\sqrt{\frac{1+S^2}{2}}\left[X(1-S^2) \mp Q(1+S^2) - 8S\right]/D_0 \tag{36}$$

with

$$D_0 = \left[X(X+4)\right]^{\frac{1}{2}}\left[4 \pm S(Q+X)\right](1-S^2), \tag{37}$$

where we have defined

$$X = V_4 / V_2 \tag{38}$$

and

$$Q = (X^2+16)^{\frac{1}{2}}. \tag{39}$$

Note that all explicit dependence on V_6 has cancelled out in this limit.

In the Harrison limit the coefficients are most conveniently expressed in terms of Harrison's polarity and covalency parameters[1,2] α_p and α_c, respectively:

$$\alpha_p = V_3/(V_2^2+V_3^2)^{\frac{1}{2}} \tag{40}$$

and

$$\alpha_c = V_2/(V_2^2+V_3^2)^{\frac{1}{2}} = (1-\alpha_p^2)^{\frac{1}{2}} \tag{41}$$

One finds

$$\left\{\begin{matrix} a_{4M} \\ a_{5M} \end{matrix}\right\} = \frac{1}{\sqrt{2}}\left[\pm\alpha_c(1-S^2)^{\frac{1}{2}} + S\alpha_p\right]/(1-S^2) \tag{42}$$
$$a_{6M} = -\frac{2}{\sqrt{2}}\sqrt{\frac{1+S^2}{2}}\,\alpha_p/(1-S^2)$$

and

$$\begin{Bmatrix} a_{6M} \\ a_{7M} \end{Bmatrix} = \frac{1}{2}\left[1 \pm \alpha_p (1-S^2)^{\frac{1}{2}}\right]\left[S\chi_{6M} + \theta\right]/(1-S^2)$$

$$a_{6M} = \sqrt{\frac{1+S^2}{2}}\left[\alpha_{6M} + S\theta\right]/(1-S^2), \tag{43}$$

where $\theta = +1$ for $M = V$ and $\theta = -1$ for $M = M'$. It is strightforward to show that all of the above results for the FH and Harrison limits are equivalent to those of Paper I in the limit $S = V_6 = 0$.

B. Physical Properties

The full effects of two-electron correlation and overlap on a wide range of physical properties can be assesed using the eigenvalues and eigenstates obtained above. We shall concentrate here, however, on only a small select number of such properties. For the purposes of comparison with HC and Paper I, we derive generalized formulas for the dielectric constant ϵ and the nuclear exchange and pseudodipolar coefficients Γ_e and Γ_{pd}, respectively. As an extension of the method, we also consider the valence-electron density, polarity of the bond and the cohesive energy.

1. Dielectric Constant

As in Paper I, the quantities ϵ, Γ_e and Γ_{pd} are most conveniently calculated in perturbation theory. Following HC and Paper I, we apply an electric field $\vec{\mathcal{E}}$ in the $+x$ direction and consider the energy shift ΔE induced in an isolated bond lying in the [111] direction. The origin of coordinates is chosen at the center of the bond and, in analogy with Eqs. (34) - (41) of Paper I, the shift in the total energy (per unit volume) of the crystal to second-order in E is just

$$\sum_{\text{bonds}} \mathcal{H}_i = -\sum_{\text{bonds}} (\vec{P}_0 \cdot \vec{\mathcal{E}}) - \frac{1}{2} \chi \mathcal{E}^2 , \tag{44}$$

where the polarization is

$$\vec{P}_0 = -(\sqrt{3}/d) \sum_{ij} \langle G | \mathcal{U}_0^{\circ} | a \rangle \vec{e}_{ij} \tag{45}$$

and the electric susceptibility is

$$\chi = -Ne^2 \sum_{M \neq G} \frac{\langle G | \mathcal{U}_\varepsilon^{\circ} | M \rangle \langle M | \mathcal{U}_\varepsilon^{\circ} | G \rangle}{E_M - E_G} . \tag{46}$$

Here $\mathcal{U}_\varepsilon^{\circ}(\vec{r}_1, \vec{r}_2) = x_1 + x_2$, $|G\rangle = |M\rangle$ is the ground state, N is the average valence-electron density, and $\vec{d}$ is the vector distance from the anion to the cation. Note that the sum in Eq. (46) runs only over the two excited singlet states, because $\mathcal{U}_\varepsilon^{\circ}$ cannot couple $|G\rangle$ to the triplet states. Using Eqs. (4) and (31), one can derive a general formula for $\langle G | \mathcal{U}_\varepsilon^{\circ} | G \rangle$ in terms of the expansion coefficients a_{iM}:

$$\begin{aligned}
\langle G | \mathcal{U}_\varepsilon^{\circ} | M \rangle = (d/\sqrt{3}) \sum_{\alpha} \beta (1-S^2)^{\frac{1}{2}} \Big\{ & (a_{5G} a_{5M} - a_{4G} a_{4M}) \\
& + \tfrac{1}{2} S \sqrt{\tfrac{2}{1+S^2}} \sum_{\alpha} \left[(a_{5\alpha} - a_{4\alpha}) a_{6M} + (a_{5M} - a_{4M}) a_{6G} \right] \Big\} \\
& - (\delta_c - \delta_a) \Big\{ (a_{5G} a_{5M} + a_{4G} a_{4M}) + a_{6G} a_{6M} / (1+S^2) \\
& + \tfrac{1}{2} S \sqrt{\tfrac{2}{1+S^2}} \sum_{\alpha} \left[(a_{5G} + a_{4G}) a_{6M} + (a_{5M} + a_{4M}) a_{6G} \right] \\
& - 2\delta_{ca} \Big\{ \tfrac{1}{2} \sum_{\alpha} \left[(a_{4G} a_{5M} + a_{5G} a_{4M}) + a_{6G} a_{6M} / (1+S^2) \right] \\
& + \tfrac{1}{2} S \sqrt{\tfrac{2}{1+S^2}} \sum_{\alpha} \left[(a_{5G} + a_{4G}) a_{6M} + (a_{5M} + a_{4M}) a_{6G} \right] \Big\} ,
\end{aligned} \tag{47}$$

where we have defined

$$\delta_n \quad (\quad) \left| \int (\quad) \chi_n \phi_n(\vec{r}) \, d\vec{r} \right| , \qquad n = a, c , \tag{48}$$

$$\gamma' = \left| 1 - (\quad) \right| \quad \tag{49}$$

and

$$\delta_{ca} \equiv -(\quad) \int \phi_c^*(\vec{r}) \chi \phi_a(\vec{r}) \, d\vec{r} \quad . \tag{50}$$

In Eq. (48) χ_n is the χ coordinate measured from the center n. The quantity $|1-(\delta_a+\delta_c)|$ is the γ' defined in Eq. (16) of HC and Eq. (36) of Paper I. The renormalization factor of $(1-S^2)^{\frac{1}{2}}$ is again such that our γ is precisely the same as that defined by HC. Note that $\delta_n d$ is just the center of gravity of the hybrid electron density $\phi_n^*(\vec{r})\phi_n(\vec{r})$. A new overlap term δ_{ca}, not considered in either HC or Paper I, has also appeared. For homopolar solids $\delta_{ca} = 0$ and $\delta_c = \delta_a$ by symmetry; for binary compounds one usually has $\delta_c > \delta_a$ and $\delta_{ca} > 0$ because of the greater spatial extent of the cation hybrid.

In the FH and Harrison limits, $\vec{P}_0$ and χ are given by particularly simple expressions. In the former case $\delta_{ca} = \delta_c = \delta_a = 0$ and one finds, as in Paper I, that only the matrix element $\langle G|\mathcal{U}_\varepsilon^0|IV\rangle$ is non-zero. Thus $\vec{P}_0 = 0$, as expected by symmetry. Using Eqs. (35) and (36), it is also straight-forward to show that

$$\epsilon = 1 - \pi\chi = 1 - \tfrac{1}{3}\pi N(\gamma e d)^2 (1/V_2 \beta), \tag{51}$$

with

$$\beta = \tfrac{1}{64} Q(Q+X)\left[32 Z + X(1-3S^2) + Q(1-S^2)\right]/(1-S^2), \tag{52}$$

where we have defined

$$Z \equiv 2V_0/V_2 . \tag{53}$$

Equation (51) has the same analytic structure as obtained in HC and Paper I, and the factor β reduces to Eq. (46) of Paper I in the limit $S = Z = 0$. In addition, $\beta = 1$ for $X = Z = 0$ and $\beta > 1$ for $Z \geq 0$ and $X \geq 0$. A further simplification is also possible. In HC the quantity V_2^{HC} is determined by fitting $E_{IV} - E_{VI}$ to the principal optical-absorption peak. If one uses the same standard to fix V_2, then one has, comparing Eq. (26) and Eq. (29) with $V_3 = 0$.

$$2V_2^{HC} = \tfrac{1}{2} V_2 \left[32 + X(1-3S^2) + Q(1-S^2)\right]/(1-S^2), \tag{54}$$

and the effect of the two-electron correlation on the HC result can be expressed in terms of the simpler factor

$$\beta' = V_2 \beta / V_2^{HC} = \tfrac{1}{16} Q(Q+X), \tag{55}$$

which depends only on X and not on either S or Z explicitly. Our calculations suggest $X \sim 1$ for the group-IV elements, in which case $\beta' \sim 1.3$. In addition, if the quantity γ is determined by fitting ϵ to experiment, then the fitted γ will be larger than the HC value by a factor of $(\beta')^{\frac{1}{2}}$.

In the Harrison limit $\langle G|\mathcal{U}_\epsilon^o|IV\rangle$ and $\langle G|\mathcal{U}_\epsilon^b|G'\rangle$ are finite and $\langle G|\mathcal{U}_\epsilon^b|V\rangle$ vanishes. Using Eqs. (29), (42), and (43) one finds in this case

$$\vec{P}_0 = \{ \quad \} \vec{r} \qquad (56)$$

and

$$\epsilon = 1 + \tfrac{4}{3}\pi N \left(\quad \right) d^3 \quad / \left(\quad \right)^{3/2}, \qquad (57)$$

where we have defined

$$\gamma^{HC} = \gamma + \left(\quad \right) \quad / \left(\quad \right)^{\frac{1}{2}} . \qquad (58)$$

Equations (56)-(58) reduce to the HC results in the limit $\delta_c = \delta_a$ and $\delta_{ca} = 0$, as was implicitly assumed in their work. Setting $S = \delta_{ca} = 0$, one recovers Eqs. (48) and (51) of Paper I for $\vec{P}_0$ and ϵ, respectively.

We should mention at this point that the vanishing of the matrix element $\langle G | \mathcal{U}_\varepsilon' | V \rangle$ only appears to be an exact result in the FH and Harrison limits. However, our calculations suggest that the additive term $|\langle G|\mathcal{U}_\varepsilon'|V\rangle|^2/(E_G - E_V)$ in Eq. (46) makes a negligibly small contribution to χ in real materials. Thus even in the general case, the correlation correction to χ^{HC} is essentially a multiplicative factor as in Eq. (55).

2. Electron Density and Polarity

The total valence-electron density in the solid is just a sum of all the individual bond densities. The bond electron density may be obtained from the two-electron ground state $|G\rangle$ in the following way. If the spatial part of the singlet basis state $|i\rangle$ is written as $\psi_i(\vec{r}, \vec{r}')$, then the electron density associated with the ground state is from Eq. (31) just

$$\rho(\vec{r}) = 2 \sum_{i,j=1,3,6} a_{iG}^* a_{jG} \int \psi_i^*(\vec{r}, \vec{r}') \psi_j(\vec{r}, \vec{r}') \, d\vec{r}' \qquad (59)$$

The factor of 2 arises because there are two electrons per bond, i.e., $\int \rho(\vec{r}) \, d\vec{r} = 2$. Also note that $\psi_i(\vec{r}, \vec{r}')$

is symmetric in $\vec{r}$ and $\vec{r}'$, so that it does not matter over which coordinate one integrates in Eq. (59). Using Eq. (4), it is simple to show that

$$f(\vec{r}) = u_a^2 \phi_a^2(\vec{r}) + u_c^2 \phi_c^2(\vec{r}) + 2 u_{ac} \phi_a(\vec{r}) \phi_c(\vec{r}) \tag{60}$$

with

$$u_a^2 = 2\alpha_{4G}^2 + a_{6G}^2/(1+S^2) + 2\sqrt{1+S^2}\, a_{4G} a_{6G} \tag{61}$$

$$u_c^2 = 2\alpha_{5G}^2 + a_{6G}^2/(1+S^2) + 2\sqrt{1+S^2}\, a_{5G} a_{6G} \tag{62}$$

and

$$u_{ac} = 2S\alpha_{4G} a_{6G} + S a_{6G}^2/(1+S^2) + \sqrt{1+S^2}\,(a_{4G} + a_{6G})\alpha_{6G}\,, \tag{63}$$

where we have noted that $\phi_a(\vec{r})$ and $\phi_c(\vec{r})$ are real. In the FH limit one finds using Eq. (36)

$$\begin{aligned} u_a^2 = u_c^2 &= 16\{Q(Q-8S)(1+S^2) + 32S^2 - [4S(Q+X) - XQ](1-S^2)\}(1-S^2)/D_b^2 \\ u_{ac}^2 &= 16\{Q(8-QS)(1+S^2) - 32S - [4(Q-X) + SXQ](1-S^2)\}(1-S^2)/D_b^2 . \end{aligned} \tag{64}$$

In the Harrison limit, on the other hand, one is led from Eq. (43) to the results

$$\left\{ \begin{matrix} u_a^2 \\ u_c^2 \end{matrix} \right\} = [(1-S\alpha_c) \pm \alpha_p(1-S^2)^{1/2}]/(1-S^2) \tag{65}$$

and

$$u_{ac}^2 = u_a u_c = (\alpha_c - S)/(1-S^2) . \tag{66}$$

For $\chi = 0$ in Eq. (64) or $\alpha_p = 0$ and $\chi_c = 1$ in Eqs. (65) and (66), $u_a^2 - u_c^2 = u_{ac}^2 = (1+S)^{-1}$, as one might expect.

We tentatively define a polarity associated with the electron density as

$$\alpha_p^G \equiv \tfrac{1}{2}\left(u_a^2 - u_c^2\right)(1-S^2)^{\frac{1}{2}} . \tag{67}$$

From Eq. (65) one clearly has $\alpha_p^G = \alpha_p$ in the Harrison limit, so that Eq. (67) is consistent with the HC concept of polarity. In the limit of no overlap, both $S = 0$ and $\phi_a(\vec{r})\phi_c(\vec{r}) = 0$ and this definition is relatively unambiguous. In the case of large overlap, on the other hand, the definition of α_p^G seems less compelling. Ultimately, an arbitrariness arises from the innumerable ways one can divide up the electron density in a periodic solid. Nevertheless, there need be no additional uncertainty in any calculation, so long as α_p^G enters solely as a definition.

The concept of polarity is also intimately connected with the polarization of the bond $\vec{P}_0$. Using Eq. (47) with $M = G$ in Eq. (45), one has in the general case

$$\vec{P}_0 = Z_p e \vec{d} , \tag{68}$$

where

$$Z_p = \gamma \alpha_p^G + \tfrac{1}{2}(\delta_c - \delta_a)\left(u_a^2 + u_c^2\right) + 2\delta_{ca} u_{ac}^2 . \tag{69}$$

The quantity $Z_p e$ is the effective charge associated with the dipole $\vec{P}_0$. It would follow, therefore, that Z_p is also a reasonable measure of polarity. However, this definition has the disadvantage of depending on the additional parameters γ, δ_a, δ_c and δ_{ca}. In HC the quantities $\delta_c - \delta_a$ and δ_{ca} are set to

zero and γ is fitted to experiment through the dielectric constant Eq. (57). The fitted γ thus adsorbs local-electric-field corrections to ϵ as well as corrections to the bond-orbital model itself. Consequently, it is not appropriate to use their γ in any definition of polarity. On the other hand, one may calculate α_p directly and compare it to α_p^{η}, and we do this in Sec. III.

We finally point out that one may, as we did in Paper I, define a polarity for each of the states $|M\rangle$ by an obvious generalization of Eqs. (59)-(67). It readily follows from Eqs. (35) and (42) that $\alpha_p^M = 0$ for all three singlet states in the FH limit and that $\alpha_p^{II} = 0$ and $\alpha_p^{V} = -\alpha_p^{G}$ in the Harrison limit. These results are in agreement with those obtained in Paper I.

3. Indirect Nuclear Interactions

To obtain generalized expressions for Γ_e and Γ'_{pd}, we again consider the magnetic interaction between an electron with spin $\frac{1}{2}\hbar\vec{\sigma}$ and a nucleus with spin $\vec{I}$. In analogy with Paper I, this interaction couples only singlet and triplet states and to second-order gives rise to an energy shift out of the ground state of

$$\Delta E = \frac{1}{E_G - E_I} \sum_{M=I,II,III} \langle G|\mathcal{U}_A|M\rangle\langle M|\mathcal{U}_A|G\rangle \quad , \tag{70}$$

where

$$\mathcal{U}_A(\vec{r}_1,\vec{r}_2) = \sum_{i=1,2}\sum_{n=a,c} \vec{I}_n \cdot \overleftrightarrow{A}_n(\vec{r}_i)\cdot\sigma(\vec{r}_i) \tag{71}$$

and

$$\overleftrightarrow{A}_n(r) = \mu_B\hbar\gamma_n\left[\frac{8\pi}{3}\delta(\vec{r})\overleftrightarrow{1} + \frac{1}{r^3}\left(3\hat{r}\hat{r} - \overleftrightarrow{1}\right)\right] . \tag{72}$$

In Eq. (72) μ_B is the Bohr magneton, γ_n is the gyromagnetic ratio and $\vec{r}$ is the electron coordinate measured relative to the nucleus n. The triplet states, as given by Eq. (1), have the form $\Phi_A(\vec{r}_1,\vec{r}_2)\chi_M$ and the sum over M in Eq. (70) can be immediately accomplished by using the sum rule

$$\sum_{M=1,0,-1} \langle \Sigma_A | \vec{\sigma}(i) | \Sigma_M \rangle \langle \Sigma_M | \vec{\sigma}(i') | \Sigma_A \rangle = (-1)^{i+i'} \overleftrightarrow{1} \tag{73}$$

Then using Eqs. (2) and (31) and noting that $\Phi_A(\vec{r}_1,\vec{r}_2)$ is antisymmetric in $\vec{r}_1$ and $\vec{r}_2$, one may express ΔE in terms of the expansion coefficients a_{ij}:

$$\Delta E = -\frac{1}{E_0} \sum_{n,n'=a,c} \theta_n \theta_{n'} \vec{I}_n \cdot \overleftrightarrow{Q}_n \cdot \overleftrightarrow{G}_1 \cdot \vec{I}_{n'} \tag{74}$$

where $\theta_a = +1$ and $\theta_c = -1$ and we have set

$$\overleftrightarrow{G}_n = \theta_n \{ \langle \phi_a | \overleftrightarrow{A}_n | \phi_a \rangle - \langle \phi_c | \overleftrightarrow{A}_n | \phi_c \rangle + (b_1^2 - b_2^2)^{-1} [\langle \phi_a | \overleftrightarrow{A}_n | \phi_a \rangle + \langle \phi_c | \overleftrightarrow{A}_n | \phi_c \rangle - 2 \langle \phi_a | \overleftrightarrow{A}_n | \phi_c \rangle] \} / (1 - S^2)^2 , \tag{75}$$

$$b_1 = \tfrac{1}{2} (\alpha_{ac} - \alpha_{ca})$$

$$b_2 = \tfrac{1}{2} (\alpha_{aa} + \alpha_{cc} + \alpha_{ac} / \sqrt{2(1+S)}) , \tag{76}$$

and

$$E_0^{-1} = \frac{2 b_2^2}{E_T - E_G} . \tag{77}$$

Equation (74) is a generalization of Eq. (62) of Paper I. In addition to S, four new overlap matrix elements have appeared in ΔE, namely, $\langle \phi_a | \overleftrightarrow{A}_a | \phi_c \rangle$

$\langle \phi_a | \overleftrightarrow{A}_c | \phi_c \rangle$, $\langle \phi_a | \overleftrightarrow{A}_c | \phi_a \rangle$, and $\langle \phi_c | \overleftrightarrow{A}_a | \phi_c \rangle$. It is not hard to show that all matrix elements of $\overleftrightarrow{A}_n$ have the form

$$\langle \phi_n | \overleftrightarrow{A}_{n'} | \phi_{n''} \rangle = \tfrac{1}{2} \mu_B \hbar \gamma_n \left[\tfrac{1}{3} \delta_{nn''}^{n'} \overleftrightarrow{\mathbb{1}} + \tfrac{1}{2} \beta_{nn''}^{n'} \overleftrightarrow{TT} \right], \quad n, n', n'' = a, c \tag{78}$$

with

$$\overleftrightarrow{TT} = 3 \hat{r}_{ac} \hat{r}_{ac} - \overleftrightarrow{\mathbb{1}}, \tag{79}$$

and where we have defined

$$\delta_{nn''}^{n'} \equiv 16\pi \langle \phi_n | \delta(\vec{r}_{n'}) | \phi_{n''} \rangle \tag{80}$$

and

$$\beta_{nn''}^{n'} \equiv \frac{5}{3} \langle \phi_n | \left(\frac{3 z_{n'}^2}{r_{n'}^5} - \frac{1}{r_{n'}^3} \right) | \phi_{n''} \rangle . \tag{81}$$

In Eq. (79) $\hat{r}_{ac}$ is a unit vector directed from the anion to the cation and in Eqs. (80) and (81) the electron coordinates $\vec{r}_{n'}$ are to be measured from the center n'. Also, the right-hand side of Eq. (81) is written for the Z axis in the direction of $\vec{r}_{ac}$. More explicit expressions for $\delta_{nn''}^{n'}$ and $\beta_{nn''}^{n'}$ in terms of the s and p components of the sp^3 hybrids are given in Sec. III and the Appendix. As expected, the non-overlap terms δ_{nn}^{n} and β_{nn}^{n} immediately reduce to Eqs. (64) and (65) of Paper I.[6] Furthermore, the tensor $\overleftrightarrow{Q}_n$ clearly has the same form as Eq. (78) with $\delta_{nn''}^{n'}$ replaced by δ_n

$$\delta_n = \Theta_n \left[\left(1 + S \frac{b_1}{b_2}\right) \delta_{aa}^{n} - \left(1 - S \frac{b_1}{b_2}\right) \delta_{cc}^{n} - 2 \frac{b_1}{b_2} \delta_{ac}^{n} \right] / (1 - S^2)^{1/2} \tag{82}$$

and $\rho_{n'}$ replaced by

$$\rho_n \rightarrow \rho_n \left[\left(1 + S\frac{b_1}{b_2}\right)\rho_{nA}^{n'} - \left(1 - S\frac{b_1}{b_2}\right)\rho_{nC}^{n'} - 2\frac{b_1}{b_2}\rho_{nC}^{n'} \right] / (1 - S^2)^{\frac{1}{2}} . \tag{83}$$

Writing out $\vec{Q}_n \cdot \vec{Q}_{n'}$ in terms of δ_n and ρ_n and noting that $\overleftrightarrow{\pi} \cdot \overleftrightarrow{\pi} = 2\overleftrightarrow{1} + \overleftrightarrow{\pi}$, we arrive at the final results

$$\Delta E = -\frac{1}{2} \sum_{n,n'=a,c} \theta_n \theta_{n'} \vec{I}_n \cdot \left[\Gamma_e^{nn'} \overleftrightarrow{1} + \Gamma_{pd}^{nn'} \overleftrightarrow{\pi} \right] \cdot \vec{I}_{n'} , \tag{84}$$

where

$$\Gamma_e^{nn'} = \mu_B^2 \hbar^2 \gamma_n \gamma_{n'} \left[\frac{1}{18} \delta_n \delta_{n'} + \frac{7}{25} \rho_n \rho_{n'} \right] / E_0 \tag{85}$$

and

$$\Gamma_{pd}^{nn'} = \mu_B^2 \hbar^2 \gamma_n \gamma_{n'} \left[\frac{1}{10} \left(\delta_n \rho_{n'} + \delta_{n'} \rho_n \right) + \frac{9}{50} \rho_n \rho_{n'} \right] / E_0 . \tag{86}$$

Equations (84)-(86) have the same analytic structure as the corresponding results obtained in Paper I, with all effects of two-electron correlation and overlap being absorbed into the quantities δ_n, ρ_n and E_0. Again we identify $\Gamma_e \equiv \Gamma_e^{ac}$ and $\Gamma_{pd} \equiv \Gamma_{pd}^{ac}$ as the nuclear exchange and pseudodipolar coefficients, respectively. We normally expect δ_n and ρ_n and consequently Γ_e and Γ_{pd} to be positive quantities, as is observed experimentally, provided

$$0 \leq b_1/b_2 \leq S \tag{87}$$

and

$$\delta_{nn}^{n} > \delta_{nn'}^{n} > \delta_{nn}^{n'}$$
$$\gamma_{nn}^{n} > \gamma_{nn'}^{n} > \gamma_{nn}^{n'} \qquad (88)$$

for $n' \neq n$. The lower limit in Eq. (87) is exact for homopolar solids, where $a_{4M} = a_{5M}$. We find Eqs. (87) and (88) obeyed for all group-IV and III-V binary compounds.

In the FH limit, Eqs. (82) and (83) simplify to

$$\delta_n = \theta_n \left[\delta_{aa}^{n} - \delta_{cc}^{n} \right] / (1-S^2)^{\frac{1}{2}}$$
$$\gamma_n = \omega_n \left[\gamma_{aa}^{n} - \gamma_{cc}^{n} \right] / (1-S^2)^{\frac{1}{2}} \quad . \qquad (89)$$

The coupling constant E_0^{-1} can be shown to be in this case

$$E_0^{-1} = \frac{1}{4V_2}\,\xi \quad , \qquad (90)$$

where

$$\xi = 64(Q+X-4S)^2(1-S^2)/\{Q(Q+X)[4-S(Q-X)]^2[2Z - X(1+S^2) + Q(1-S^2)]\} \quad , \qquad (91)$$

which reduces to Eq. (72) of Paper I in the limit $S=Z=0$. Also, $\xi > 1$ for $Z > 0$ and/or $X > 0$, and $\xi = 1$ for $X = Z = 0$. If V_2^{HC} and V_2 are related by Eq. (54), then the HC value of E_0^{-1} is enhanced by the factor

$$\xi' = V_2^{HC}\,\xi / V_2 = \tfrac{1}{4}\left[2Z + X(1-3S^2) + Q(1-S^2)\right]\xi/(1-S^2) \quad , \qquad (92)$$

which unlike β' is a function of S and Z as well as X . In Fig. 1 we have plotted ξ' vs X for $Z = 0$ and several values of S . Clearly, ξ' is a sensitive

function in the region of physical interest: $S \sim 0.6$, $\chi \sim 1.0$. This sensitivity results primarily from the energy denominator in Eq. (77), which can vanish for sufficiently large χ .

In the Harrison limit

$$\delta_n = \theta_n \{ [(1-S^2)^{1/2} + S(\alpha_p/\alpha_c)] \delta_{aa}^n - [(1-S^2)^{1/2} - S(\alpha_p/\alpha_c)] \delta_{cc}^n - 2(\alpha_p/\alpha_c)\delta_{ac}^n \} / (1-S^2) , \tag{93}$$

with a similar expression for γ_n , and

$$E_b^{-1} = \frac{1}{4} V_2^2 / (V_2^2 + V_3^2)^{3/2} . \tag{94}$$

Equation (94) agrees with Eq. (73) of Paper I, but note that for $\delta_{cc}^a = \delta_{aa}^c = \delta_{ac}^c = \delta_{ca}^c = 0$ and $S \neq 0$. We do not recover our previous formulas for $\Gamma_e^{nn'}$ and $\Gamma_{Pd}^{nn'}$. Contrary to our original expectations, all terms involving S cannot simply be absorbed into V_2 and V_3 . Both $\Gamma_e^{nn'}$ and $\Gamma_{Pd}^{nn'}$ are multiplied instead by a factor of $[1 - S^2(\alpha_p/\alpha_c)^2/(1-S^2)]/(1-S^2)$ in this limit.

4. Cohesive Energy

To obtain the cohesive energy, one needs both the binding energy of the (two) bond electrons in an anion-cation pair and the binding energy of the (eight) valence electrons in separated atoms. The latter can be written as

$$E_{atoms} = \begin{cases} 2(\varepsilon_{sa}^{HF} + \varepsilon_{sc}^{HF}) + (2+\Delta Z)\varepsilon_{pa}^{HF} + (2-\Delta Z)\varepsilon_{pc}^{HF} & \Delta Z = 0,1,2 \\ 2\varepsilon_{sa}^{HF} + \varepsilon_{sc}^{HF} + 5\varepsilon_{pa}^{HF} & \Delta Z = 3 \end{cases} \tag{95}$$

where $\Delta Z = 0$ for group IV, $= 1$ for III-V, $= 2$ for II-VI and $= 3$ for

I-VII elements. Also in Eq. (95) ε_{sn}^{HF} and ε_{pn}^{HF} are defined as the binding energies of the s and p electrons of atom n. We use the superscript HF here because in practice it is convenient to take ε_{sn}^{HF} and ε_{pn}^{HF} to be Hartree-Fock free-atom eigenvalues, although in principle this need not be assumed. The corresponding binding energy of two bond electrons is just our ground-state energy E_G plus the electrostatic energy of the compensating nuclei:

$$E_{bond} = E_G + e^2/d = \varepsilon_a^{HF} + \varepsilon_c^{HF} + E_{ol} + E_G^0 \quad , \tag{96}$$

where we have defined the hybrid energies

$$\varepsilon_n^{HF} = \frac{1}{4}\left(\varepsilon_{sn}^{HF} + 3\varepsilon_{pn}^{HF}\right) , \qquad n = a, c , \tag{97}$$

and the electrostatic overlap energy

$$E_{ol} = -K + e^2/d + \Delta\varepsilon_a + \Delta\varepsilon_c \quad , \tag{98}$$

with

$$\Delta\varepsilon_n = \varepsilon_n - \varepsilon_n^{HF} \quad , \qquad n = a, c . \tag{99}$$

Both Harrison[1] and HC discarded E_{ol} in their treatments of the cohesive energy. However, for the case of large overlap this is not justified, since we expect $\Delta\varepsilon_n$ to be small and negative and K to be significantly larger than e^2/d.

Using Eqs. (95) and (96), the cohesive energy (per atom pair) is just

$$\begin{aligned} E_{coh} &= E_{atoms} - 4E_{bond} \\ &= -4E_G^0 - 4E_{ol} - E_{prep} - E_{hybrid} \quad , \end{aligned} \tag{100}$$

where E_{prom} is the promotion energy defined by Harrison[1]

$$E_{prom} = \begin{cases} (7+\Delta z)V_1' + (4-\Delta z)V_1'' & \Delta z = 0, 1, 2 \\ 3V_1' + V_1'' & \Delta z = 3 \end{cases} \tag{101}$$

with

$$V_1^{\alpha} \equiv \frac{1}{4}\left(\varepsilon_{p\alpha}^{HF} - \varepsilon_{s\alpha}^{HF}\right), \qquad \alpha = a, c, \tag{102}$$

and E_{trans} is the transfer energy

$$E_{trans} = \Delta z\left(\varepsilon_c^{HF} - \varepsilon_a^{HF}\right). \tag{103}$$

Both Harrison[1] and HC took the transfer energy to be $2\Delta z\, V_3$. From Eqs. (19), (27) and (99), however, one can see that this is only formally valid here if $u_a = u_c$, $\Delta\varepsilon_a = \Delta\varepsilon_c$ and $S = 0$. In the FH limit with $E_{trans} = 0$ and $E_{prom} = 8V_1''$, one has

$$E_{coh} = 4\left[(4V_2^2 + V_4^2)^{\frac{1}{2}} - 2S V_2 - V_4 + V_6\right] - 4E_{sl} - 8V_1''. \tag{104}$$

In the Harrison limit, on the other hand, one obtains

$$E_{coh} = 4\left[2(V_2^2 + V_3^2)^{1/2} - 2S V_2\right] - 4E_{sl} - E_{prom} - E_{trans}. \tag{105}$$

For $E_{sl} = 0$ and $E_{trans} = 2\Delta z\, V_3$, this result agrees with Eq. (34) of HC.

Physically, we may interpret the various contributions to E_{coh} as follows. The promotion energy is the energy required to promote each valence electron from its atomic s or p orbital to an sp^3 hybrid orbital. The transfer energy is the energy required to transfer ΔZ electrons from the anion to the cation at infinite separation, so that the four hybrid orbitals on each atom contain one electron. The atoms are then brought together and bond orbitals are formed from the overlapping hybrids. Occupation of the bond orbitals returns an energy $-(E_{\sigma}^{o} + E_{ol})$ per bond. Equation (100) thus correctly includes all intrabond contributions to the cohesive energy. To be sure, there are neglected interbond contributions, as there are to all properties one calculates with the bond-orbital model, but we certainly expect these to be of lesser importance. In HC the possible importance of a van der Waals interaction between the bonds was argued, but this was introduced in an ad hoc fashion to explain their calculated negative values of E_{coh}. In contrast, our calculations suggest that there is no fundamental difficulty in understanding the cohesive energy of tetrahedrally-bonded solids in terms of Eq. (100) alone, although the precise results one obtains are somewhat sensitive to the details of the calculation.

III. QUANTITATIVE APPLICATIONS

A. Parameters of the Two-electron Model

We now consider a detailed application of the formalism described above to real semiconductors. Our analysis will be considerably more complete than that given in Paper I, as we seek to understand quantitatively both the relative importance of the various parameters which enter the two-electron theory and the effect of overlap and correlation on the predictions of the one-electron theory. We must first establish a procedure for evaluating the basic parameters of the two-electron model. We are guided here both by the experience of HC and the fundamental limitations of a bond-orbital approach. One must recognize the approximate nature of any bond-orbital theory, so that the difficult task of a complete first-principles analysis is not really warranted. On the other hand, one can reasonably expect the theory to produce correct orders of magnitude and significant trends for a wide range of physical properties. Thus it seems desirable to fit only enough parameters to provide a proper scaling to experiment.

Of the various parameters which enter our two-electron model, one may separate out those which depend self-consistently on the full Hamiltonian of the crystal, and consequently are difficult to calculate accurately, and those which depend only on the specification of the hybrid wavefunctions. In the former category are the quantities V_{2_0}, $\Delta\varepsilon_A$ and $\Delta\varepsilon_C$. Both V_{20} and $\Delta\varepsilon_A + \Delta\varepsilon_C$ enter the covalent energy V_2, while the polar energy V_3 depends upon the

difference $\Delta\varepsilon_c - \Delta\varepsilon_a$. Following HC, we fit V_2 to the principal optical-absorption peak E_2 for each of the group IV elements. From Eq. (54) with $V_3 = 0$

$$V_2 = \frac{1}{2}\left\{\left[2V_2^{HC} - V_4(1-3S^2)/(1-S^2)\right]^2 - V_4^2\right\}^{1/2}, \tag{106}$$

which is easily evaluated once S and V_4 are specified. It is then assumed that V_2 is constant for an isoelectronic sequence (e.g., Ge, GaAs, etc.) and that values for skew compounds are given by the appropriate geometric means of the group-IV values. The quantity V_3 was fitted by HC to the experimental dielectric constant of each binary compound through Eq. (57). This is less convenient in the present case because V_3 enters our theory through the rather complicated cubic equation (24). We have chosen instead to make the assumption

$$\Delta\varepsilon_c - \Delta\varepsilon_a = 0 \tag{107}$$

and then to calculate V_3 as

$$V_3 = \frac{1}{2}\left[\left(\varepsilon_c^{HC} - \varepsilon_a^{HC}\right) - \frac{1}{2}\left(U_a - U_c\right)\right] / \left(1-S^2\right)^{1/2}. \tag{108}$$

Since $|\Delta\varepsilon_n/\varepsilon_n|$ is small, one may reasonable expect Eq. (108) to be a good approximation. From Eq. (18) it is clear that the term $\frac{1}{2}(U_a - U_c)$ will reduce the magnitude of V_3, so that normally $V_3 < \frac{1}{2}\left(\varepsilon_c^{HF} - \varepsilon_a^{HF}\right)$, as was found empirically by HC. Interestingly, the two exceptions to Eq. (18), namely BP and BAs, are the compounds for which HC inferred negative values of V_3^{HC} from their fitting procedure. From Table I it can be seen that the quantity $\frac{1}{2}\left(\varepsilon_c^{HF} - \varepsilon_a^{HF}\right)$ does become much smaller for BP and BAs than for the rest of the III-V compounds.

However, this effect is offset by the change in sign of the term $-\frac{1}{2}(U_a - U_c)$, so that normal positive values of V_3 result from Eq. (108).

The remaining parameters V_4, V_5 and V_6 are functions of the one-center integrals U_n and the two-center integrals S, K, H_n and J. All of these integrals depend only on the hybrid wavefunctions $\phi_n(\vec{r})$, so that we also choose to calculate these quantities directly. In the spirit of the bond-orbital model, we construct our hybrids from the appropriate Hartree-Fock free-atom s and p wavefunctions. We shall not entertain the very difficult question of exactly which atomic orbitals constitute an optimum basis set, but rather we treat our choice as an additional assumption to be tested. Choosing $\hat{r}_{ac} \quad \hat{x}$, one can write

$$\phi_n(\vec{r}_n) = \frac{1}{2\sqrt{4\pi}}\left[R_{sn}(r_n) + 3\theta_n R_{pn}(r_n)\frac{z_n}{r_n}\right], \tag{110}$$

where $\vec{r}_n$ is the electron coordinate measured relative to the center n and $R_{sn}(r_n)$ and $R_{pn}(r_n)$ are assumed to be positive as $r_n \to \infty$. Free-atom Hartree-Fock s and p radial wavefunctions, $r_n R_{sn}(r_n)$ and $r_n R_{pn}(r_n)$, as well as the corresponding term values ε_s^{HF} and ε_p^{HF}, have been calculated and tabulated by Mann[7] for the entire Periodic Table. The use of such atomic tables is convenient, but it does restrict one to consideration of compounds formed out of group III, IV and V elements, since the p states of elements in groups I and II are unoccupied and are not usually calculated. The details of evaluating U_n, S, K, H_n and J in terms of the hybrids defined by Eq. (110) are discussed in the Appendix. Briefly, U_n can be written as a sum of the F and G integrals defined and calculated by Mann[7], as shown in Eq. (77) of Paper I. As a test of our numerical procedures, we have also evaluated these

F and G integrals directly from Mann's wavefunctions. Our calculated values of U_n are listed in Table I and are to be compared with those given in Table I of Paper I, which were inferred from Mann's tables. The agreement is better than 0.1%. The two-center integrals S and H_n, on the other hand, are most easily calculated by expanding the sp^3 hybrid from one site in terms of spherical harmonics centered on the second site. Similarly K can be evaluated by expanding the Coulomb potential arising from one hybrid electron density about the second site. In both cases, this procedure leads to a finite series of one-dimensional integrals. This same type of expansion method applied to the exchange integral J, however, leads to an infinite series of terms, which must be truncated. Tests of our procedures in the case of hydrogen $1s$ orbitals, where exact results are known[8], suggest that we calculate S, H_n and K to an accuracy of better than 1%, but that we may underestimate J by a few percent.

Values of S, K and V_4 that we have computed for the twenty group-IV elements and group-IV and III-V binary compounds are listed in Table II, together with values of V_2 obtained from Eq. (106) and V_3 obtained from Eq. (108). The two-center Coulomb integral K decreases with increasing bond length, as expected. The overlap integral S, on the other hand, tends to be constant, although AlN, GaN and InN have somewhat smaller values than the rest. For the solids listed in Table II, one has approximately $K \sim (1+S)\, e^2/d \sim 1.6\, e^2/d$. The constancy of S and the simple dependence of K on bond length give V_4 its expected covalent behavior. The large magnitude of S, however, alters the relationship of V_2 and V_2^{HC} anticipated in Paper I. For $S = 0$ Eq. (106) demands that $V_2 < V_2^{HC}$, but in our case $S^2 > \frac{1}{3}$ and we calculate $V_2 > V_2^{HC}$. For the group-IV elements $X = 2\,V_4/V_2 = 0.77$ for C, $= 1.08$ for Si, $= 1.10$ for Ge, and $= 1.13$ for Sn.

As mentioned in Sec. II, our calculated values of V_5 and V_6 always turn out to be small in comparison with V_3 and V_4, respectively. Specifically, we find

$$0.11 \geq V_5 \geq -0.02 \text{ eV} \qquad (111)$$

$$|V_5 / V_3| < 0.075$$

and

$$0.27 \geq V_6 \geq -0.02 \text{ eV} \qquad (112)$$

$$|V_6 / V_4| < 0.11$$

for all twenty solids considered here. In view of the large overlap of the sp^3 hybrids, the uniform smallness of V_5 and V_6 is indeed remarkable, and we have found no simple explanation for these results. The magnitudes of V_5 and V_6 are actually comparable to the numerical uncertainty in these quantities. For the sake of conceptual simplicity we shall set $V_5 = V_6 = 0$ in our subsequent analysis. Note that with V_2 fit to experiment and V_5 and V_6 set to zero, values for the integrals H_{ss} and J are no longer required.

Having established values for the basic parameters of our two-electron model, we may quantitatively solve the cubic equation (24) for the singlet-state eigenvalues. We have done this and the values of E_M^0, defined by Eq. (23), are given in Table III, together with the triplet-state eigenvalues

$$E_T^0 = 2S V_2 - 2S^2 V_4 / (1 - S^2) \qquad (113)$$

for the twenty solids under consideration. The corresponding eigenstate expansion coefficients a_{4M}, a_{5M} and a_{6M}, as calculated from Eqs. (32)-(34), are listed in Table IV. Also, in Table III we compare our theoretical values for

the principal optical-absorption peak $E_2 = E_{IV} - E_G$ with both the HC predictions, $E_2^{HC} = 2\left[(V_2^{HC})^2 + (V_3^{HC})^2\right]$, and the experimental E_{2A} and E_{2B} sub-peaks as given by Phillips.[9] Because E_2 for the group-IV elements represents a fitting parameter, only the results for the binary compounds offer a test of the theory. Both our E_2 and E_2^{HC} for these latter materials agree with the available experimental data to within 12%. Our E_2 tend to agree best with E_{2B} and E_2^{HC} with E_{2A}, but the differences do not appear to be significant. It is important to stress, however, that our E_2, in contrast to E_2^{HC}, include no direct experimental data for the binary compounds.

B. Computed Properties

With the information given in Tables I-IV, we may systematically study the physical properties discussed in Sec. II. We begin with the dielectric constant, for which we need the additional quantities γ, δ_a, δ_c, and δ_{ca}. All of these parameters are readily calculable from the hybrid wavefunctions (110) and the values we have obtained are given in Table V. For the group-IV elements, the dielectric constnat is given directly in terms of γ, V_2^{HC} and β' by Eqs. (51) and (55). From Table II we calculate $\beta' = 1.23$ for C, $= 1.35$ for Si, $= 1.36$ for Ge, and $= 1.37$ for Sn. For the binary compounds, the coupling matrix elements $\langle G|\mathcal{U}_\mathcal{E}^\circ|M\rangle$ must be computed from Eq. (47). As remarked in Sec. II, the term $|\langle G|\mathcal{U}_\mathcal{E}^\circ|M\rangle|^2/(E_G - E_{IV})$ dominates the sum in Eq. (46) for the susceptibility χ. We find

$$|(E_G - E_{IV})/(E_G - E_V)||\langle G|\mathcal{U}_\mathcal{E}^\circ|V\rangle/\langle G|\mathcal{U}_\mathcal{E}^\circ|IV\rangle|^2 < 0.01 \qquad (114)$$

in all cases. Finally, we scale our calculated values of χ for the group-IV elements in the manner of HC. Specifically, we replace γ in Eq. (51) by $\lambda_n\gamma$

and determine a λ_n for each row of the Periodic Table by fitting ϵ to experiment. We obtain $\lambda_n = 2.02$ for C, $= 2.22$ for Si, $= 2.56$ for Ge, and $= 2.11$ for Sn. For the binary compounds, we multiply our calculated χ by $\lambda_a \lambda_c$, where λ_a and λ_c are the appropriate values of λ_n for the anion and cation rows. Again as in the optical-absorption calculation and in contrast to HC, we do not use any direct experimental data for the binary compounds in determining the dielectric constant for these materials. In Fig. 2 we have plotted our theoretical dielectric constants versus the best available experimental values[10] for the twenty materials under consideration here. The agreement with experiment is within 12% for the binary compounds and, together with our results for E_2, lends strong support to our method of determining parameters.

We next consider the valence-electron density and the polarity of the bond. We have made a full evaluation of the single-bond electron density, as given by Eq. (60), in the cases of Ge and $GaAs$. These results are plotted in Figs. 3 and 4, respectively. There is a broad peak in the electron density at the center of the bond in Ge and a somewhat sharper peak near the As site in $GaAs$. In both cases the bond is elongated perpendicular to the bond axis. The remaining peaks and valleys in the core regions result from the oscillations in the s and p atomic wavefunctions due to their orthogonality to the inner core states. We have also repeated these calculations in the Harrison limit using Eqs. (65) and (66) with $\alpha_c = \alpha_c^{HC}$ and $\alpha_p = \alpha_p^{HC}$, the HC values of the covalency and the polarity. Interestingly, the results obtained are very close to those of the full calculations; in the bonding region the differences in both cases are on the order of 1%. This is consistent with the fact that we calculate $\alpha_p^2 \approx \alpha_p^{HC}$ for $GaAs$ as well as Ge (see Table V) and suggests that the electron-

density coefficients u_a, u_c and u_{ac} are determined primarily by the polarity. As can be seen from Eqs. (65) and (66), the latter is exactly true in the Harrison limit.

To obtain the total electron density in the crystal, one must superimpose the individual single-bond densities. We have done this along a bond axis in both Ge and GaAs and the results are plotted in Figs. 5 and 6. The density near the center of the bond is increased only slightly by the overlap, but there is a significant increase in electron density in the back-bonding regions. For comparison we have also plotted in Figs. 5 and 6 the corresponding results of Walter and Cohen[11] obtained via the local-empirical-pseudopotential method.[12] Their calculated densities are qualitatively similar to ours in the bonding and back-bonding regions, although clearly they find a higher electron density in the center of the bond than we do.

An accurate experimental determination of the valence-electron density has been made in the case of Si, although not in either Ge and GaAs. It has been pointed out[14] that the Walter and Cohen calculation for Si yields the magnitude of the central peak to within 7% of experiment. In view of Fig. 5, it is of interest to consider what modifications in our sp^3 hybrids are required to in increase $\rho(\vec{r})$ in the center of the bond. From Eqs. (60), (65), (66) and (110), the electron density at the midpoint of the bond in a group-IV element is to a good approximation

$$\rho(d/2) = \frac{1}{4\pi}\left[R_s(d/2) + 3R_p(d/2)\right]^2/(1+S)\,. \tag{115}$$

Free-atom wavefunctions lead to a value of 0.063 a.u. for $\rho(d/2)$ in Si, as compared with the value of 0.102 a.u. found experimentally.[13] However, by smoothly contracting the tails of $R_s(r)$ and $R_p(r)$ beyond $r = d/2$, one can

easily increase $\rho(d/2)$ to the required height[15], as we have verified in a computer experiment. It seems clear, therefore, that valuable information about the shape of the hybrids can be extracted from an accurate knowledge of the electron density in the bonding region. This matter will be pursued elsewhere.

Our defined polarity α_p^G has been evaluated for each of the sixteen binary compounds considered here and these results, together with the corresponding values of α_p^{HC}, are given in Table V. For the non-nitrate Al, Ga and In compounds, we find α_p^G approximately constant (0.51 to 0.56), which is roughly in accord with α_p^{HC} (0.44 to 0.54). For the corresponding nitride compounds, however, we consistently calculate $\alpha_p^G \sim \frac{1}{2}\alpha_p^{HC}$. In addition, we find $\alpha_p^G < \alpha_p^{HC}$ for SiC and BN and $\alpha_p^G > \alpha_p^{HC}$ for BP and BAs. These trends can be qualitatively understood in terms of our computed values of V_3 and V_4. Generally speaking, α_p^G increases with increasing V_3 and decreases with increasing V_4. We calculate $V_3 < V_3^{HC}$ and $V_3 < V_4$, and consequently relatively small values of α_p^G, for SiC and all of the nitride compounds. For the remaining compounds, on the other hand, we obtain $V_3 > V_3^{HC}$ with $V_4 \cong V_3$ for BP and BAs and $V_3 < V_4$ for the others.

For comparison with α_p^G and α_p^{HC}, we have also listed in Table V our calculated values of Z_p, as defined by Eq. (69). Generally, there does not seem to be a simple correlation between Z_p and either α_p^G or α_p^{HC}. We find $Z_p \cong \alpha_p^G$ for SiC and the nitrides, but $Z_p < \alpha_p^G$ for the rest. Interestingly, however, there is a qualitative correlation between $(\delta_c - \delta_a)$ and α_p^{HC}. In particular, the trend of decreasing α_p^{HC} with increasing mean atomic number in the B, Al, Ga and In series (except for AlSb) are all reflected in

$(\delta_c - \delta_a)$. In this regard, note that $(\delta_c - \delta_a)$ measures the relative spatial extent of the cation and anion hybrids, while α_p^G measures the relative weighting of these hybrids in the electron density.

Let us now move on to consider the nuclear exchange and pseudodipolar coefficients. To evaluate Eqs. (85) and (86) for Γ_e and Γ'_{pd}, one needs values for the matrix element $\mathcal{S}_{nn''}^{n'}$ and $\mathcal{P}_{nn''}^{n'}$. Equation (80) for $\mathcal{S}_{nn''}^{n'}$ is easily evaluated in terms of the hybrids defined by Eq. (110):

$$\mathcal{S}_{nn''}^{n'} = \begin{cases} [R_{sn}(0)]^2 & n = n' = n'' \\ R_{sn}(0)\,[R_{sn''}(d) + 3R_{pn''}(d)] & n = n' \neq n'' \\ [R_{sn}(d) + 3R_{pn}(d)]^2 & n = n'' \neq n' \end{cases} \tag{116}$$

For free-atom wavefunctions $R_{sn}(0) >> [R_{sn}(d) + 3R_{pn}(d)]$ and consequently $\mathcal{S}_{nn}^{n} >> \mathcal{S}_{nn'}^{n} >> \mathcal{S}_{nn}^{n'}$. Specifically, we find

$$\begin{aligned} |\mathcal{S}_{nn'}^{n} / \mathcal{S}_{nn}^{n}| &< 0.10 \\ |\mathcal{S}_{nn}^{n'} / \mathcal{S}_{nn}^{n}| &< 0.01 \end{aligned} \tag{117}$$

in all cases. The situation for $\mathcal{P}_{nn''}^{n'}$ is slightly more complicated. Only $\mathcal{P}_{nn}^{n}$ has a simple formula in terms of the hybrids:

$$\mathcal{P}_{nn}^{n} = \int_0^\infty R_{pn}^2(r)\,\frac{dr}{r} \,. \tag{118}$$

To evaluate the overlap terms one must use the wavefunction-expansion techniques discussed in the Appendix. Specific formulas for $\mathcal{P}_{nn'}^{n}$ and $\mathcal{P}_{nn}^{n'}$ are given there. Quantitatively, we find

$$|\beta^{n}_{nn'}/\beta^{n}_{nn}| < 0.27$$
$$|\beta^{n'}_{nn}/\beta^{n}_{nn}| < 0.18 \quad , \tag{119}$$

although the upper limits are only approached in the case of BN . Typically the ratios are much smaller. For completeness we have included all four overlap terms, $\delta^{n}_{nn'}$, $\delta^{n'}_{nn}$, $\beta^{n}_{nn'}$ and $\beta^{n'}_{nn}$, in calculating Γ_e and Γ'_{pd} . Values of Γ_e and Γ_{pd} have been determined both in the Harrison limit, using V_2^{HC} and V_3^{HC} to evaluate Eqs. (93) and (94), and with the full theory, using the data listed in Tables III and IV to evaluate b_1 , b_2 and E_0 . These results are presented in Table VI together with the best available experimental data. Note that the values of Γ_e and Γ_{pd} in the Harrison limit are larger (except for $In N$) than the corresponding ones given in Table II of Paper I. This is due primarily to the appearance of the overlap matrix element S in Eq. (93), as was discussed in Sec. II. Also, as expected from Fig. 1, the effect of two-electron correlation is to enhance Γ_e and Γ_{pd} in all cases. The magnitude of the enhancement, however, shows rather complicated trends depending both on bond length and polarity. In the group-IV elements, $\xi' = 2.04$ for C , $= 3.30$ for Si and Ge , and $= 3.53$ for Sn .

We have not included any additional scaling factors in the theoretical numbers listed in Table VI. This does not appear to be important in the case of Γ_{pd}, but clearly we overestimate the magnitudes of Γ_e , although the trends are correct. We have made an approximate least-squares fit to the six non-zero experimental values of Γ_e using a functional form

$$\Lambda_a \Lambda_c \Gamma_e \tag{120}$$

where Λ_2 and Λ_3 are constants which depend only on row number in the Periodic Table and the Γ_e are the full-theory values given in Table VI. We have thereby determined scaling factors Λ_n appropriate to each row: $\Lambda_n = 0.71$ for the Si row, $= 0.57$ for the Ge row and $= 0.64$ for the Sn row. As with the scaling factor λ_n in the dielectric constant, Λ_n increases with increasing atomic number. Note, however, that $\lambda_n > 1$ while $\Lambda_n < 1$.

In Paper I we noted the following relationship between the dielectric constant and the nuclear exchange coefficient in the Harrison limit (without overlap):

$$\epsilon - 1 = C \Gamma_e / d^4 , \tag{121}$$

where C is independent of V_2 and V_3 and depends only on intra-atomic parameters. [See the discussion pertaining to Eq. (74) of Paper I.] This motivated us to plot experimental values of $(\epsilon - 1)$ against the known experimental values of $\Gamma_e / \Gamma_{dd} d^4 = \Gamma_e / (\gamma_a \gamma_c \hbar^2 d)$, and we found a rather striking linear relationship in the series InP, $InAs$ and $InSb$. Since that time, experimental determinations of Γ_e and Γ_{pd} for GaP, as well as new measurements on $GaAs$, have been made by Cueman and Soest[16], allowing them to make a similar plot for the Ga series. They have found a good linear relationship for that series too; both sets of experimental data are shown in Fig. 7. We are now in a position to make a meaningful theoretical plot of $(\epsilon - 1)$ vs. $\Gamma_e / \Gamma_{dd} d^4$. Using our calculated values of ϵ from Fig. 3 and our full-theory values of Γ_e from Table VI, we have done this in Fig. 8 for all the III-V compounds. Approximate linear trends can be seen in the In and Ga series, as well as the Al series, for the heaviest three compounds. To examine the origin of this

behavior, we repeated the procedure in the Harrison limit. In this case, the linear behavior was improved slightly in the I_n series, worsened slightly in the G_a series, and was destroyed in the A_l series. Keeping only the most dominant terms in $\delta_{nn'}^{n'}$ and $\gamma_{nn''}^{n''}$, one has in the Harrison limit

$$\hbar^2 \gamma_a \gamma_c C \sim \left[\frac{\lambda_a \lambda_c}{\delta_{aa}^{a} \delta_{cc}^{c} \beta'} \right] \left[\frac{18\sqrt{3} (\gamma e)^2 (1-S^2)^2}{(1-S^2) - S^2 (\alpha_p^{HC}/\alpha_c^{HC})^2} \right] , \qquad (122)$$

where by construction $(\lambda_a \lambda_c / \beta')^{1/2} \gamma$ is the HC fitted value of γ. Now for the heavier G_a and I_n compounds β', γ, S, α_p^{HC} and α_c^{HC} are rather constant. This implies that for a given cation series

$$\lambda_a / \delta_{aa}^{a} \sim \text{constant} . \qquad (123)$$

Evaluation of Eq. (123) gives 0.0155 for Sb, 0.0163 for As, and 0.0311 for P. The higher value for P is consistent with Fig. 8, where the points for Al P, Ga P and In P all lie above the straight line defined by the corresponding As and Sb compounds.

A comparison of Table II of Paper I and Table VI shows that our full treatment of overlap and two-electron correlation has had only a modest impact on the important ratio Γ_{pd}/Γ_e. Moreover, in no case has that ratio been increased significantly, which, as pointed out in Paper I, is necessary to simultaneously reconcile Γ_{pd} and Γ_e with experiment. It now seems clear that Γ_{pd}/Γ_e is dominated by the ratio $\beta_{nn}^{n}/\delta_{nn}^{n}$, which in turn is a direct property of the s and p wavefunctions which make up the hybrid. Interestingly, we have found in the case of Si that the latter ratio can be increased if the tails of the free-atom wavefunctions are contracted in the manner necessary to account for the electron

density in the center of the bond. This matter bears further investigation in the case of binary compounds.

As our final application, we turn to the cohesive energy. For the group IV elements, it is instructive to rewrite Eq. (104) as

$$E_{coh} = 8(1-S)\,V_2^{HC} - 4E_{corr} - 4E_{bl} - E_{pro} \quad , \tag{124}$$

where $-4E_{corr}$ is the explicit contribution of two-electron correlation to the cohesive energy. Using Eq. (106) and comparing Eqs. (104) and (124), one has (with $V_6 = 0$)

$$E_{corr} = 2(1-2S^2)\,V_4/(1-S^2) - 2S(V_2^{HC} - V_2) \quad . \tag{125}$$

As desired, $E_{corr} = 0$ for $V_4 = 0$. Unfortunately, a complete evaluation of Eq. (124) requires the uncertain quantity $\Delta\mathcal{E}_a + \Delta\mathcal{E}_c$. Because an accurate evaluation of $\Delta\mathcal{E}_n$ is quite difficult, we calculate only the remaining terms. Specifically, we replace E_{bl} in Eq. (124) with

$$E_{bl}^{\circ} = -K + e^2/d \tag{126}$$

and use our calculated values of V_1^n , V_2 , V_4 , S and K to evaluate E_{coh} and its components. The results are listed in Table VII together with the experimental values of the cohesive energy. Note that our calculated E_{coh} is less than experiment but positive in each case. This is consistent with small negative values of $\Delta\mathcal{E}_n$, as we expect theoretically. Also note that $-4E_{bl}^{\circ}$ makes a large positive contribution and $-4E_{corr}$ a smaller, but non-negligible, negative contribution to E_{coh} . We may contrast this with the calculation of E_{coh} made by HC. They, of course, neglected both E_{bl} and E_{corr} . Quantitatively, these omissions were partly compensated for by their use of smaller values of S (a constant value of 0.5) and a scaling factor of 0.8 multiplying E_{pro}. Their prescription gives a rather fortuitous value of $E_{coh} = 11.1$ eV for C , but negative values of -2.72 for Si , -3.94 for Ge , and -3.01 for Sn .

We have determined empirical values of $\Delta\mathcal{E}_n$ for each group-IV element by fitting to the experimental cohesive energy:

$$\Delta\mathcal{E}_n^{fit} = (E_{coh} - E_{coh}^{expt})/8 . \qquad (107)$$

As can be seen from Table VII, the magnitudes of the $\Delta\mathcal{E}_n^{fit}$ are reasonable. The irregular variation from element to element is questionable and no doubt partly reflects the fact that our theoretical model is best for a large-band-gap material like C . In any case, we have used Eq. (107) to extend the calculation of E_{coh} to the binary compounds. We have assumed that $\Delta\mathcal{E}_c + \Delta\mathcal{E}_a$ is a covalent quantity and have used the appropriate arithemetic mean of the group-IV values for each compound together with a direct calculation of the remaining terms in Eq. (100). The results are plotted against the known experimental cohesive energies in Fig. 9. The comparison is not as favorable as with E_2 and ϵ , but positive values are found in all cases except $In\,N$.

IV. CONCLUSIONS

We have presented here the full formal theory of the two-electron bond-orbital model, extended its application, and extensively compared and contrasted it with Harrison's one-electron bond-orbital model. Both the analytic formulas given in Sec. II and the parameters listed in Tables I-V can be used to treat many additional physical properties, including those considered by Harrison and co-workers with the one-electron model. Our work here has shown that two-electron correlation effects are significant in the dielectric constant, the nuclear exchange and pseudodipolar coefficients, and the cohesive energy, but perhaps not in the valence electron density, where the polarity and the shape of sp^3 hybrid wavefunctions are the dominant quantities. In $\epsilon - 1$, Γ_e and Γ_{rd} , however, the effect of correlation is essentially multiplicative and is hidden to some extent if scaling factors, a la HC, are used to achieve quantitative agreement with experiment. Nevertheless, it is encouraging that we have been successful here by actually fitting less parameters to experiment that did HC. An interesting and potentially important area for additional work is in the optimization of the sp^3 hybrid wavefunctions and in the impact this has on calculated parameters such as V_3 , V_4 , β_{nn}^n and $\beta_{nn}^{n'}$.

ACKNOWLEDGMENTS

We are indebeted to J. A. Van Vechten for sending us his latest table of experimental dielectric constants and to J. F. Soest and M. K. Cueman for sharing their experimental results with us prior to publication.

APPENDIX

We present here useful formulas for quantitatively evaluating the two-electron integrals U_{nn} and K and the other two-center integrals S, δ_{cA}, $P^{n}_{nn'}$ and $P^{n'}_{nn}$ discussed in Secs. II and III. Central to the evaluation of U_{nn} and K is the standard expansion

$$\frac{1}{|\vec{r}-\vec{r}'|} = 4\pi \sum_{\ell,m} \frac{1}{2\ell+1} \frac{r_<^{\ell}}{r_>^{\ell+1}} Y^*_{\ell m}(\vec{r}') Y_{\ell m}(\vec{r}) \quad , \tag{A1}$$

where $Y_{\ell m}(\vec{r})$ is the usual spherical harmonic and $r_<$ ($r_>$) is the lesser (greater) of r and r'. We choose the z axis to be in the bond direction such that the cation is located a distance $+d\hat{z}$ from the anion. Then only the $m = 0$ component of Eq. (A1) (as well as any other similar expansion) will contribute to the integrals of interest, and one may work in terms of the Legendre polynomials P_ℓ:

$$Y_{\ell 0}(\vec{r}) = \sqrt{\frac{2\ell+1}{4\pi}} P_\ell(\cos\theta) \, . \tag{A2}$$

In terms of the P_ℓ, the $\underline{S}p^3$ hybrid wavefunctions take the form

$$\phi_n(\vec{r}) = \frac{1}{2\sqrt{4\pi}} \left[R_{sn}(r) P_0(\cos\theta) + 3\theta_n R_{pn}(r) P_1(\cos\theta) \right] , \tag{A3}$$

where $P_0(x) = 1$, $P_1(x) = x$, and $\theta_\alpha = +1$ and $\theta_\zeta = -1$, as above. Using Eqs. (A1) and (A3), the Coulomb potential arising from an $\leq p^3$ - hybrid electron density can be written

$$V_n(\vec{r}) = \int \phi_n(\vec{r}') \frac{e^2}{|\vec{r} - \vec{r}'|} \phi_n(\vec{r}') \, d\vec{r}'$$

$$= \frac{1}{4}\left[Z^0_{ss}(r) + 9 Z^0_{pp}(r) + 2\theta_n Z^1_{sp}(r) P_1(\cos\theta) + \frac{6}{5} Z^2_{pp}(r) P_2(\cos\theta) \right] \frac{e^2}{r} \quad \text{(A4)}$$

where

$$Z^k_{\ell\ell'}(r) = \int_0^r R_{\ell n}(r') \frac{r'^k}{r^k} R_{\ell' n}(r') r'^2 dr' + \int_r^\infty R_{\ell n}(r') \frac{r^{k+1}}{r'^{k+1}} R_{\ell' n}(r') r'^2 dr' . \quad \text{(A5)}$$

From Eqs. (A3) and (A4), one then has

$$U_n = \int \phi_n(\vec{r}) V_n(\vec{r}) \phi_n(\vec{r}) \, d\vec{r}$$

$$= \frac{1}{16}\left[F^0_{ss} + 9 F^0_{pp} + 6 F^0_{sp} + 4 G^1_{sp} + \frac{36}{25} F^2_{pp} \right] , \quad \text{(A6)}$$

where $F^k_{\ell\ell'}$ and $G^k_{\ell\ell'}$ are the integrals defined by Mann[7]:

$$F^k_{\ell\ell'} = \int_0^\infty R_{\ell n}(r) \frac{e^2 Z^k_{\ell\ell'}(r)}{r} R_{\ell n}(r) r^2 dr \quad \text{(A7)}$$

$$G^k_{\ell\ell'} = \int_0^\infty R_{\ell n}(r) \frac{e^2 Z^k_{\ell\ell'}(r)}{r} R_{\ell' n}(r) r^2 dr . \quad \text{(A8)}$$

To evaluate K, one can expand $V_c(\vec{r})$ in spherical harmonics centered on the anion. This type of expansion technique is discussed in detail by Löwdin.[17] Again only the $m = 0$ component of the expansion is required and one can write

$$V_c(\vec{r}-\vec{d}) = \frac{1}{4} \sum_{k=0}^{\infty} B_c^k(d,r) P_k(\cos\theta) , \tag{A9}$$

where $\vec{r}$ is measured from the anion and

$$B_c^k(d,r) = \beta_{sso}^k(d,r) + 9\beta_{ppo}^k(d,r) - 2\beta_{sp_1}^k(d,r) + \frac{6}{5}\beta_{pp_2}^k(d,r) \tag{A10}$$

with

$$\beta_{\ell\ell'k'}^k(d,r) = \frac{2k+1}{2dr} \int_{|d-r|}^{(d+r)} \frac{e^2 Z_{\ell\ell'}^{k'}(r')}{r'} P_{k'}\left(\frac{r^2-r'^2-d^2}{2dr'}\right) P_k\left(\frac{r^2-r'^2+d^2}{2dr}\right) r'dr' \tag{A11}$$

Then one finds

$$\begin{aligned} K &= \int \phi_a(\vec{r})\, V_c(\vec{r}-\vec{d})\, \phi_a(\vec{r})\, d\vec{r} \\ &= \frac{1}{16} \int_0^{\infty} \Big\{ [R_{sa}(r)]^2 B_c^0(d,r) + R_{sa}(r) R_{pa}(r) B_c^1(d,r) \\ &\qquad + [R_{pa}(r)]^2 \left[9 B_c^0(d,r) + \frac{6}{5} B_c^2(d,r)\right] \Big\} r^2 dr . \end{aligned} \tag{A12}$$

To compute the remaining integrals, one must use an expansion analagous to Eq. (A9) for the $\underline{s}\underline{p}^3$ hybrid wavefunction:

$$\phi_n(\vec{r}+\Theta_n\vec{d}) = \frac{1}{2}\sum_{k=0}^{\infty}\sqrt{\frac{2k+1}{4\pi}}\,A_n^k(d,r)\,P_k(\cos\theta)\,, \tag{A13}$$

where

$$A_n^k(d,r) = \alpha_{sn}^k(d,r) + \sqrt{3}\,\Theta_n\,\alpha_{pn}^k(d,r) \tag{A14}$$

with

$$\alpha_{\ell n}^k(d,r) = \frac{2\pi}{dr}\sqrt{\frac{2k+1}{4\pi}}\sqrt{\frac{2\ell+1}{4\pi}}\int_{|d-r|}^{(d+r)} R_{\ell n}(r')\,P_\ell\left(\frac{r^2-r'^2-d^2}{2dr'}\right)P_k\left(\frac{r^2-r'^2+d^2}{2dr}\right)r'dr'. \tag{A15}$$

Formulas for S, δ_{ca} and $\gamma_{nn'}^n$ in terms of the $A_n^k(d,r)$ follow immediately:

$$S = \frac{1}{4}\int_0^\infty \left[R_{sa}(r)\,A_c^0(d,r) + \sqrt{3}\,R_{pa}(r)\,A_c^1(d,r)\right]r^2dr\,, \tag{A16}$$

$$\delta_{ca} = \frac{1}{2}S - \frac{1}{4d}\int_0^\infty \left\{\frac{\sqrt{3}}{3}R_{sa}(r)\,A_c^1(d,r) + R_{pa}(r)\left[A_c^0(d,r) + \frac{2\sqrt{5}}{5}A_c^2(d,r)\right]\right\} r^3dr \tag{A17}$$

and

$$\gamma_{nn'}^n = \int_0^\infty \left\{\frac{\sqrt{5}}{6}R_{sn}(r)\,A_{n'}^2(d,r) + \Theta_n R_{pn}(r)\left[\frac{\sqrt{3}}{3}A_{n'}^1(d,r) + \frac{3\sqrt{7}}{14}A_{n'}^3(d,r)\right]\right\}\frac{dr}{r} \tag{A18}$$

Finally, a formula for $\rho^{n,n'}_{n,n}$ may be derived by making two expansions of the form A13:

$$\rho^{n,n'}_{n,n} = \frac{1}{8} \sum_{k,k'} (2k+1)^{1/2} (2k'+1)^{1/2} \int_0^\infty A^{k}_{n,n}(d,r)\, A^{k'}_{n',n}(d,r)\, \frac{dr}{r} \times \int_{-1}^{1} P_2(x)\, P_k(x)\, P_{k'}(x)\, dx \,. \tag{A19}$$

In this case an infinite, but rapidly convergent, series is obtained. For each value of k' there are one to three values of k which give finite contributions to the series. In our calculations we have accumulated terms up to $k=3$ and $k'=3$.

We omit results for the remaining Coulomb integrals H_n and J, as these quantities subsequently drop out of analysis given in Sec. III. A formula for H_n can be developed by using Eq. (A4) and a single expansion of the form A13. In the case of J a double expansion as in Eq. (A19) is required and an infinite series is obtained.

REFERENCES

1. W. A. Harrison, Phys. Rev. B 8, 4487 (1973). References to earlier work are given here and in Ref. 2.
2. W. A. Harrison and S. Ciraci, Phys. Rev. B 10, 1516 (1974).
3. See, for example, S. T. Pantelides and W. A. Harrison, Phys. Rev. B 11, 3006 (1975).
4. C. Huang, J. A. Moriarty, A. Sher and R. A. Breckenridge, Phys. Rev. B 12, 5395 (1975).
5. L. M. Falicov and R. A. Harris, J. Chem. Phys. 51, 3153 (1969).
6. Our current notation differs slightly from that of Paper I. The quantities ε_{n0}, V_{20}, β_{nn}^{n} and γ_{nn}^{n} were denoted as ε_n', V_2, β_n^2 and γ_n, respectively, in Paper I.
7. J. B. Mann, Los Alamos Scientific Laboratory Reports Nos. LA-3690 and LA-3691 (1967) (unpublished).
8. J. C. Slater, Quantum Theory of Molecules and Solids, Vol. 1 (McGraw-Hill, New York, 1965).
9. J. C. Phillips, Bands and Bonds in Semiconductors (Academic, New York, 1973), p. 169.
10. J. A. Van Vechten, private communication. A refined version of Table III of J. A. Van Vechten, Phys. Rev. 182, 891 (1969).
11. J. P. Walter and M. L. Cohen, Phys. Rev. B 4, 1877 (1971).
12. In this method only the pseudo-electron density is calculated and all structure in the core region is consequently absent.

13. Y. W. Yang and P. Coppens, Solid State Commun. 15, 1555 (1974).

14. J. R. Chelikowsky and M. L. Cohen, Phys. Rev. Lett. 33, 1339 (1974). These authors also report that non-local pseudopotential corrections to the method of Ref. 11 are necessary to explain the detailed shape of the experimental bond density in Si.

15. This is consistent with the experience of quantum chemists on simple diatomic molecules such as H_2. See, for example, Ref. 8.

16. M. K. Cueman and J. F. Soest, Phys. Rev. B (to be published).

17. P. O. Löwdin, Adv. Phys. 5, 1 (1956).

TABLE I. Intra-atomic parameters for the group-III, -IV and -V elements obtained from the free-atom Hartree-Fock term values and wave-functions of Mann (Ref. 7). Energies are given in eV, while δ_{nn}^{n} and β_{nn}^{n} are given in a.u.

Element	$-\varepsilon_n^{HF}$	V_1^n	U_n	δ_{nn}^{n}	β_{nn}^{n}
B	9.68	1.26	13.95	17.7	0.776
Al	6.96	1.25	9.27	29.6	1.09
Ga	7.14	1.47	9.37	87.2	2.89
In	6.56	1.19	8.43	123	4.46
C	13.14	2.08	17.62	35.0	1.66
Si	9.38	1.80	11.34	48.1	2.03
Ge	9.28	1.96	10.96	120	4.73
Sn	8.33	1.57	9.63	160	6.75
N	16.92	3.09	21.22	60.5	2.02
P	11.95	2.42	13.27	7.13	3.27
As	11.46	2.48	12.36	157	6.85
Sb	10.11	1.97	10.66	200	9.23

TABLE II. Intrabond parameters for the group-IV elements and the group-IV and III-V binary compounds. The quantity V_2 was obtained by fitting to experiment, while S, K, V_3 and V_4 were calculated using Hartree-Fock free-atom term values and wavefunctions, as described in the text. All energies are given in eV; the bond length d is given in Å.

Material	d	S	K	V_2	V_3	V_4
C	1.54	0.648	14.70	6.54	0.0	2.52
Si	2.35	0.668	9.83	2.53	0.0	1.36
Ge	2.44	0.659	9.46	2.42	0.0	1.33
Sn	2.80	0.661	8.37	1.99	0.0	1.12
SiC	1.88	0.627	11.95	4.07	0.40	2.08
BN	1.57	0.608	14.18	6.54	2.27	2.70
BP	1.97	0.663	11.65	4.07	1.74	1.75
BAs	2.07	0.656	11.14	3.98	1.71	1.77
AlN	1.89	0.517	11.27	4.07	2.33	2.71
AlP	2.36	0.633	9.58	2.53	1.93	1.41
AlAs	2.43	0.645	9.34	2.47	1.93	1.26
AlSb	2.66	0.659	8.68	2.24	1.63	1.14
GaN	1.94	0.513	11.13	3.98	2.25	2.83
GaP	2.36	0.629	9.58	2.47	1.84	1.44
GaAs	2.45	0.637	9.28	2.42	1.83	1.25
GaSb	2.65	0.654	8.70	2.19	1.54	1.15

TABLE II (cont'd.)

InN	2.15	0.470	10.16	3.61	2.25	2.99
InP	2.54	0.602	8.96	2.24	1.86	1.48
InAs	2.61	0.617	8.75	2.19	1.86	1.33
InSb	2.81	0.644	8.24	1.99	1.59	1.12

Table III. Relative singlet and triplet eigenvalues $E_M^0 = E_M - (c_a + c_c - K)$ for the twenty solids considered in the text, where $E_G^0 = E_{IV}^0$ and $E_T^0 = E_{I,II,III}^0$. Also listed are the theoretical predictions of the E_2 optical-absorption peak both from the present work, $E_2 = E_{IV}^0 - E_G^0$, and from the work of Harrison and Ciraci (Ref. 2), E_2^{HC}. All energies are in eV.

Material	E_G^0	E_T^0	E_{IV}^0	E_V^0	Theory $E_2^0 = E_{IV}^0 - E_G^0$	Theory E_2^{HC}	Experiment[a] E_{2A}	Experiment[a] E_{2b}
C	-2.32	4.82	9.87	24.32	12.2 [b]	12.2 [c]	12.2	12.2
Si	-0.50	1.19	3.91	9.98	4.41[b]	4.40[c]	4.40	4.40
Ge	-0.50	1.15	3.81	9.54	4.31[b]	4.30[c]	4.3	4.3
Sn	-0.38	0.89	3.13	7.88	3.52[b]	3.52		
SiC	-1.25	2.33	6.56	15.63	7.80	7.98	8.3	
BN	-3.33	4.78	9.95	24.87	13.3	13.4		
BP	-1.81	2.65	6.04	16.22	7.85	7.32	6.9	
BAs	-1.78	2.55	5.96	15.89	7.73	7.24		
AlN	-2.46	2.23	6.69	17.08	9.32	9.07		
AlP	-1.72	1.32	3.80	11.28	5.52	4.99		
AlAs	-1.80	1.39	3.64	10.96	5.44	4.85		
AlSb	-1.46	1.20	3.30	9.83	4.76	4.68	4.25	4.6
GaN	-2.26	2.06	6.92	16.90	9.18	9.26		
GaP	-1.59	1.22	3.76	11.02	5.35	5.11	5.27	5.74
GaAs	-1.71	1.38	3.60	10.65	5.30	4.93	4.85	5.33
GaSb	-1.36	1.14	3.26	9.57	4.61	4.31	4.1	4.5

Table III. (cont'd.)

InN	-2.13	1.70	6.61	15.96	8.74	8.54		
InP	-1.56	1.02	3.48	10.41	5.04	4.84	4.8	5.1
InAs	-1.64	1.07	3.31	10.12	4.95	4.58	4.5	5.0
InSb	-1.39	0.98	2.97	9.01	4.36	4.09[c]	4.08	

[a] Reference 9

[b] Fit to E_2^{HC}, as described in the text.

[c] Fit to experiment E_{2A}

Table IV. Expansion coefficients entering Eq. (31) for the singlet eigenstates M = VI (the ground state), M = IV and M = V of the twenty semiconductors considered in the text.

Material	M=VI			IV			V		
	a_{4M}	a_{5M}	a_{6M}	a_{4M}	a_{5M}	a_{6M}	a_{4M}	a_{5M}	a_{6M}
C	0.167	0.167	0.736	0.928	-0.928	0	-1.44	-1.44	2.33
Si	0.100	0.100	0.841	0.950	-0.950	0	-1.53	-1.53	2.47
Ge	0.103	0.103	0.838	0.940	-0.940	0	-1.49	-1.49	2.39
Sn	0.097	0.097	0.847	0.942	-0.942	0	-1.50	-1.50	2.41
SiC	0.198	0.084	0.781	0.990	-0.817	-0.200	-1.30	-1.43	2.15
BN	0.402	0.020	0.653	1.11	-0.574	-0.642	-1.06	-1.48	1.97
BP	0.465	-0.061	0.635	1.23	-0.512	-0.865	-1.21	-1.71	2.33
BAs	0.459	-0.058	0.641	1.22	-0.508	-0.855	-1.17	-1.68	2.27
AlN	0.448	-0.015	0.658	1.10	-0.357	-0.814	-0.680	-1.32	1.38
AlP	0.643	-0.120	0.494	1.26	-0.218	-1.24	-0.889	-1.65	1.92
AlAs	0.680	-0.121	0.451	1.27	-0.202	-1.30	-0.920	-1.70	2.00
AlSb	0.659	-0.131	0.480	1.30	-0.238	-1.28	-1.00	-1.75	2.14
GaN	0.428	-0.017	0.678	1.10	-0.358	-0.800	-0.675	-1.31	1.36
GaP	0.619	-0.121	0.520	1.25	-0.231	-1.21	-0.886	-1.63	1.89
GaAs	0.655	-0.113	0.476	1.26	-0.224	-1.25	-0.904	-1.66	1.95
GaSb	0.632	-0.128	0.508	1.29	-0.259	-1.24	-0.998	-1.72	2.11

Table IV. (cont'd.)

InN	0.420	-0.010	0.695	1.07	-0.310	-0.789	-0.563	-1.26	1.16
InP	0.626	-0.118	0.516	1.22	-0.179	-1.22	-0.761	-1.55	1.67
InAs	0.667	-0.122	0.471	1.24	-0.163	-1.28	-0.796	-1.60	1.76
InSb	0.674	-0.134	0.466	1.28	-0.188	-1.31	-0.911	-1.69	1.98

Table V. Calculated parameters related to the dielectric constant and the polarization of the bond, as discussed in the text. The quantity α_p^{HC} is the value of polarity assigned by Harrison and Ciraci (Ref. 2).

Material	δ_c	δ_a	$\delta_c-\delta_a$	$2\delta_{ca}$	Z_p	α_p^G	α_p^{HC}	γ
C	0.279	0.279	0.0	0.0	0.0	0.0	0.0	0.581
Si	0.265	0.265	0.0	0.0	0.0	0.0	0.0	0.633
Ge	0.257	0.257	0.0	0.0	0.0	0.0	0.0	0.646
Sn	0.259	0.259	0.0	0.0	0.0	0.0	0.0	0.643
SiC	0.331	0.229	0.102	0.098	0.14	0.08	0.39	0.565
BN	0.334	0.228	0.116	0.053	0.24	0.27	0.41	0.539
BP	0.274	0.275	-0.001	-0.040	0.20	0.35	0.0	0.602
BAs	0.261	0.275	-0.014	-0.057	0.19	0.35	0.0	0.615
AlN	0.390	0.189	0.201	0.110	0.34	0.34	0.59	0.492
AlP	0.312	0.229	0.083	0.054	0.39	0.53	0.47	0.593
AlAs	0.303	0.234	0.069	0.037	0.40	0.55	0.44	0.606
AlSb	0.277	0.251	0.026	0.004	0.36	0.54	0.54	0.628
GaN	0.363	0.184	0.179	0.114	0.33	0.32	0.62	0.528
GaP	0.299	0.229	0.070	0.050	0.38	0.51	0.52	0.607
GaAs	0.288	0.233	0.055	0.034	0.38	0.54	0.50	0.621
GaSb	0.266	0.252	0.014	-0.001	0.34	0.52	0.44	0.638
InN	0.372	0.166	0.206	0.156	0.36	0.31	0.64	0.523
InP	0.315	0.213	0.102	0.096	0.41	0.52	0.58	0.591
InAs	0.307	0.218	0.089	0.080	0.42	0.56	0.53	0.604
InSb	0.285	0.237	0.048	0.044	0.39	0.56	0.51	0.625

TABLE VI. Nuclear exchange and pseudodipolar coefficients, Γ_e and Γ_{pd}, for the twenty solids considered in the text in units of the direct dipole-dipole interaction coefficient Γ_{dd}. The theoretical results refer to our calculations done in both the Harrison limit and with the full two-electron formalism described in the text.

Material	Γ_e/Γ_{dd} Theory Harrison	Γ_e/Γ_{dd} Theory Full	Γ_e/Γ_{dd} Expt.	Γ_{pd}/Γ_{dd} Theory Harrison	Γ_{pd}/Γ_{dd} Theory Full	Γ_{pd}/Γ_{dd} Expt.	Γ_{pd}/Γ_e Theory Harrison	Γ_{pd}/Γ_e Theory Full	Γ_{pd}/Γ_e Expt.
C	0.043	0.087		0.0068	0.0139		0.160	0.160	
Si	0.846	2.79		0.130	0.427		0.153	0.153	
Ge	6.00	19.8		0.860	2.84		0.143	0.143	
Sn	19.7	69.5		3.04	10.7		0.154	0.154	
SiC	0.120	0.435		0.0187	0.0681		0.155	0.157	
BN	0.022	0.055		0.0034	0.0076		0.154	0.137	
BP	0.161	0.203		0.0254	0.0386		0.158	0.190	
BAs	0.404	0.568		0.0628	0.103		0.155	0.180	
AlN	0.077	0.273		0.0087	0.0322		0.113	0.118	
AlP	0.412	0.684		0.0619	0.102		0.150	0.150	
AlAs	1.20	1.54		0.170	0.214		0.142	0.139	
AlSb	1.56	3.15	~0.0[a]	0.233	0.469		0.149	0.149	

TABLE VI (cont'd.)

GaN	0.185	0.917		0.0218	0.107		0.118	0.117	
GaP	0.913	1.97	0.14[b]	0.140	0.303	0.20[b]	0.154	0.154	1.43
GaAs	2.69	4.26	0.73[b]	0.388	0.623	0.65[b]	0.144	0.146	0.89
GaSb	5.07	8.80	1.89[a]	0.768	1.36		0.151	0.154	
InN	0.277	2.01		0.0325	0.246		0.117	0.122	
InP	1.50	4.00	~0.55[c]	0.228	0.608	~1.0[c]	0.152	0.152	~1.8
InAs	4.71	8.72	2.06[a]	0.673	1.24		0.143	0.143	
InSb	9.18	15.6	5.28[a]	1.38	2.33		0.150	0.149	

[a] R. K. Sundfors, Phys. Rev. 185, 458 (1969).

[b] Reference 16

[c] M. Engelsberg and R. F. Norberg, Phys. Rev. B 5, 3395 (1972).

Table XII. Cohesive energy per atom pair and its components for the group - IV elements in eV. The quantities E^0_{coh} and E_{coh} are our calculated values of the cohesive energy without and with the correlation energy E_{corr}, respectively, as discussed in the text. The quantity $\Delta\epsilon_n^{fit}$ is the value of $\Delta\epsilon_n$ necessary to fit E_{coh} to E_{coh}^{expt}.

Material	$8(1-S)V_2^{HC}$	$-4\,E_{corr}$	$-4\,E^0_{o\ell}$	$-E_{pro}$	E^0_{coh}	E_{coh}	E_{coh}^{expt}	$\Delta\epsilon_n^{fit}$
C	17.18	-7.88	21.44	-16.64	22.0	14.1	14.7	-0.075
Si	5.84	-3.84	14.84	-14.40	6.28	2.44	9.28	-0.855
Ge	5.87	-3.87	14.24	-15.68	4.43	0.56	7.74	-0.898
Sn	4.77	-3.23	12.92	-12.56	5.13	1.90	6.24	-0.542

FIGURE CAPTIONS

Fig. 1 Correlation enhancement factor ξ' defined by Eq. (92) for the nuclear exchange and pseudodipolar coefficients of homopolar solids as a function of $X = 2V_4/V_2$ with $V_6 = 0$.

Fig. 2 Two-electron bond-orbital-model values of the dielectric constant ϵ for sixteen binary compounds plotted against the best available experimental values (Ref. 10). No experimental data exists for BP, BAs or InN and the estimates of Van Vechten (Ref. 10) have been used instead.

Fig. 3 Single-bond electron density for Ge as calculated from Eq. (60) using free-atom Hartree-Fock wavefunctions and the a_{iq} given in Table IV.

Fig. 4 Single-bond electron density for $GaAs$ as calculated from Eq. (60) using free-atom Hartree-Fock wavefunctions and the a_{iq} given in Table IV. The As nucleus is on the right.

Fig. 5 Profile of the total valence electron density in Ge along a bond axis, obtained by superimposing single-bond densities (Fig. 3) in the solid. The corresponding local-empirical-pseudopotential calculation of Walter and Cohen (Ref. 11) is shown for comparison (dashed line). The small arrows indicate the positions of the nuclei.

Fig. 6 Profile of the total valence electron density in $GaAs$ along a bond axis, obtained by superimposing single-bond densities

(Fig. 4) in the solid. The corresponding local-empirical-pseudopotential calculation of Walter and Cohen (Ref. 11) is shown for comparison (dashed line). The small arrows indicate the positions of the nuclei with As on the right.

Fig. 7 Experimental values of $\epsilon - 1$ vs. experimental values of $\Gamma_e / \Gamma_{dd}\, d^4$ for the seven III-V compounds on which data is available. The linear trends in the In and Ga series are to be compared against the theoretical predictions shown in Fig. 8.

Fig. 8 Theoretical values of $\epsilon - 1$ vs. theoretical values of $\Gamma_e / \Gamma_{dd}\, d^4$ for fifteen III-V compounds, as calculated from the two-electron bond-orbital model. The corresponding experimental results, as known, are plotted in Fig. 7.

Fig. 9 Two-electron bond-orbital-model values of the cohesive energy E_{coh} for sixteen binary compounds plotted against the known experimental values. References to the experimental data are given in the caption of Fig. 11 of Ref. 2.

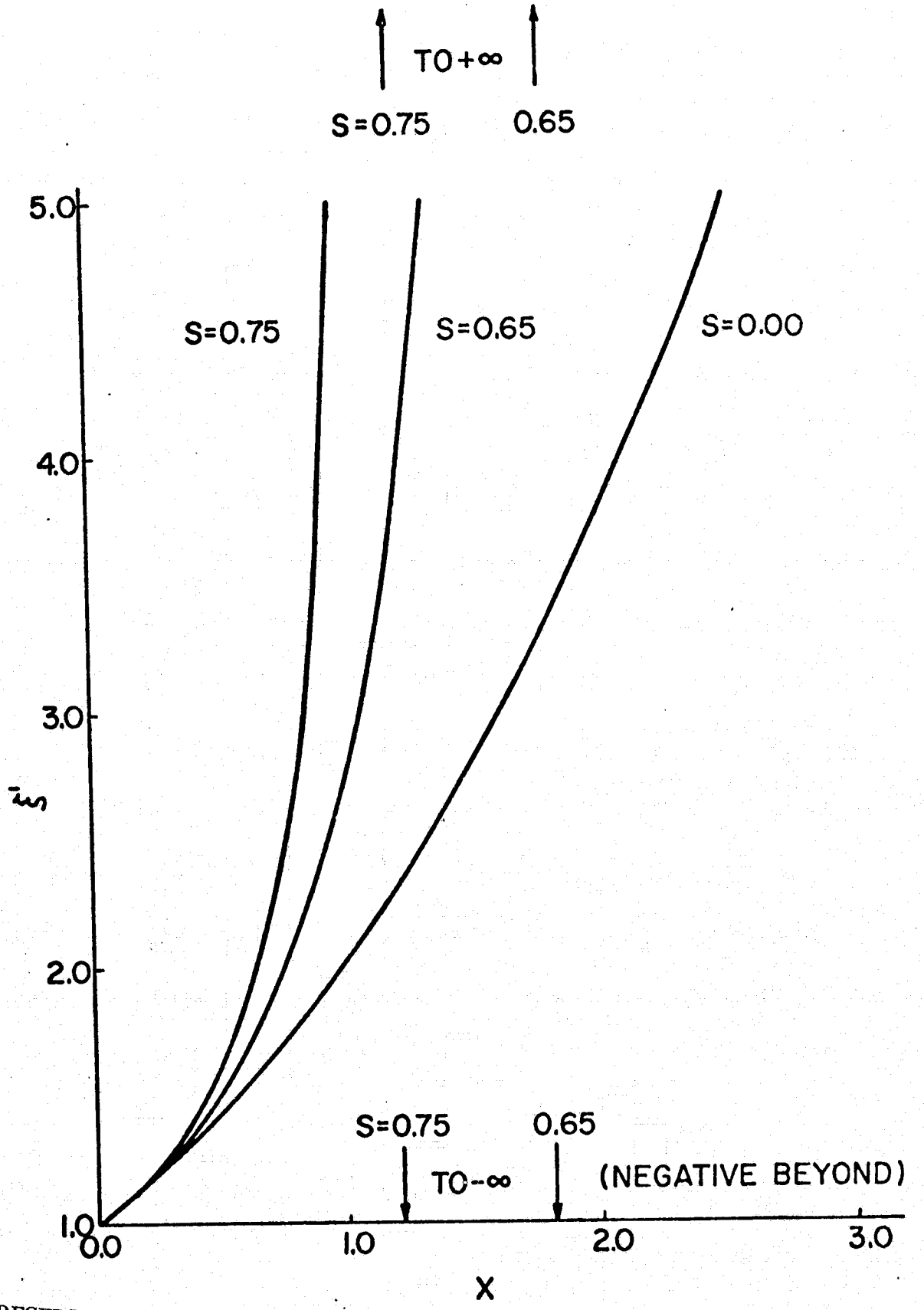

PRECEDING PAGE BLANK NOT FILMED

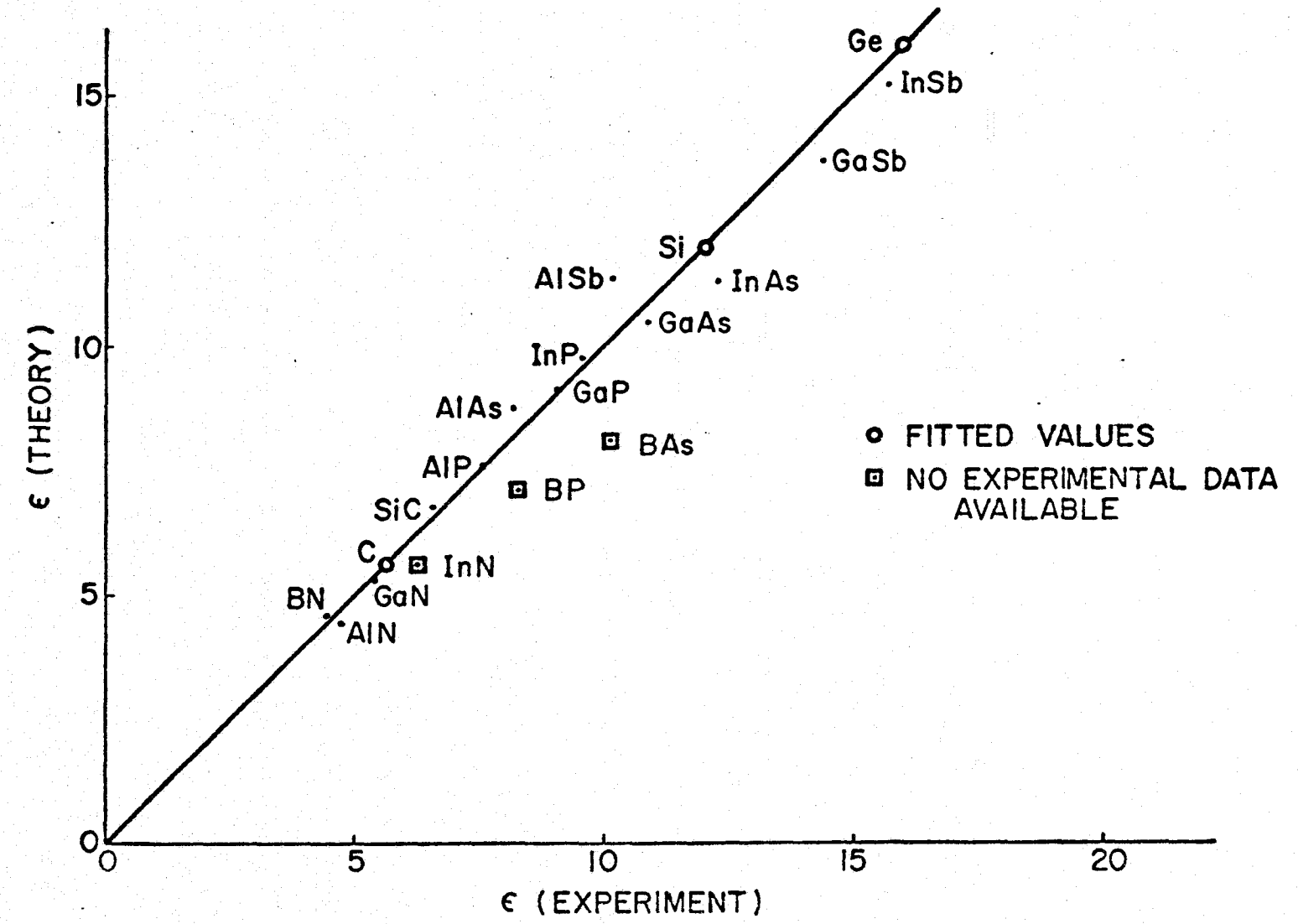
Ge
InSb
GaSb
Si
AlSb
InAs
GaAs
InP
GaP
AlAs
BAs
AlP
BP
SiC
C
InN
BN
GaN
AlN
FITTED VALUES
NO EXPERIMENTAL DATA AVAILABLE
ϵ (THEORY)
ϵ (EXPERIMENT)
0
5
10
15
20

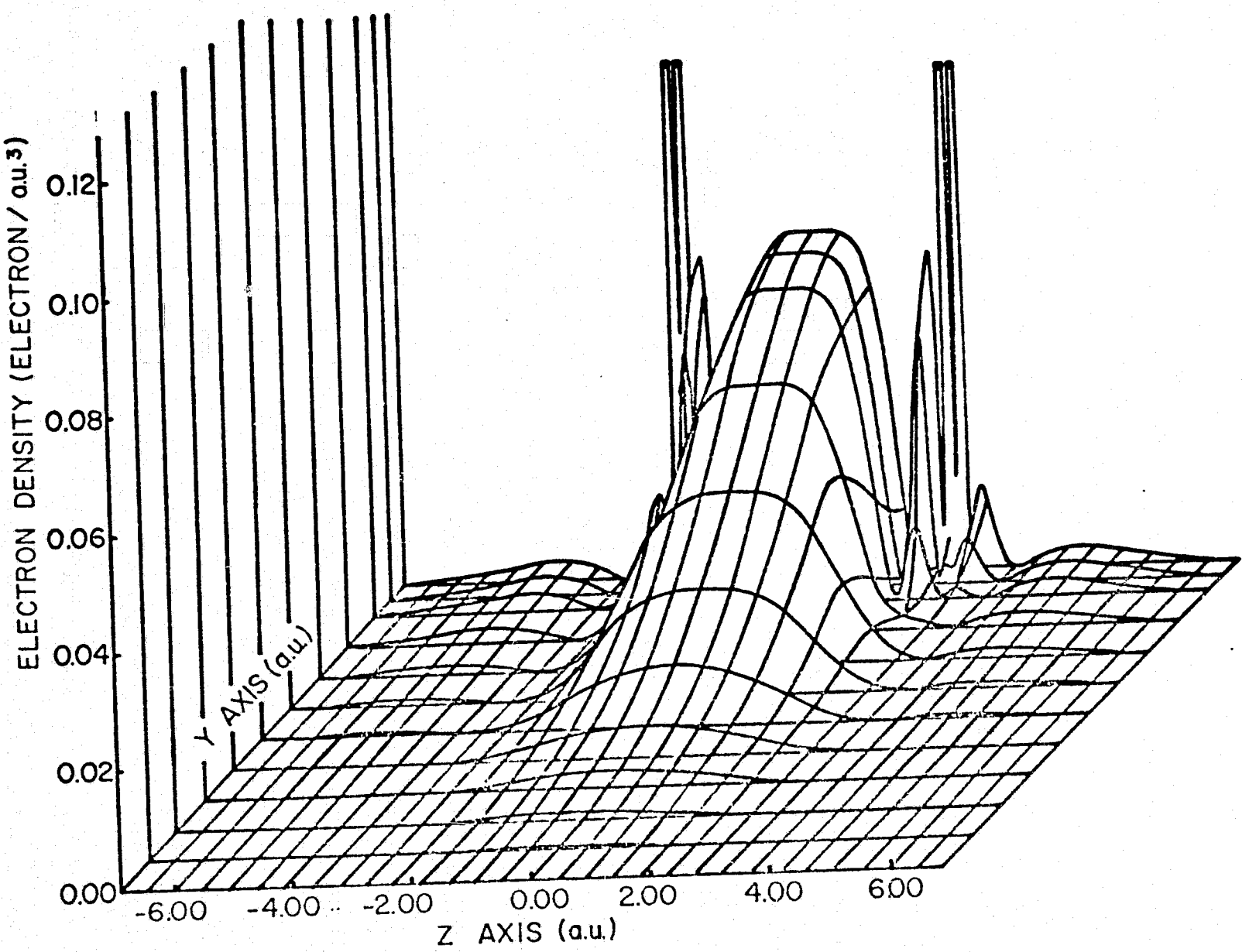
ELECTRON DENSITY (ELECTRON/ a.u.3)
0.12
0.10
0.08
0.06
0.04
0.02
0.00
Y AXIS (a.u.)
-6.00
-4.00
-2.00
0.00
2.00
4.00
6.00
Z AXIS (a.u.)

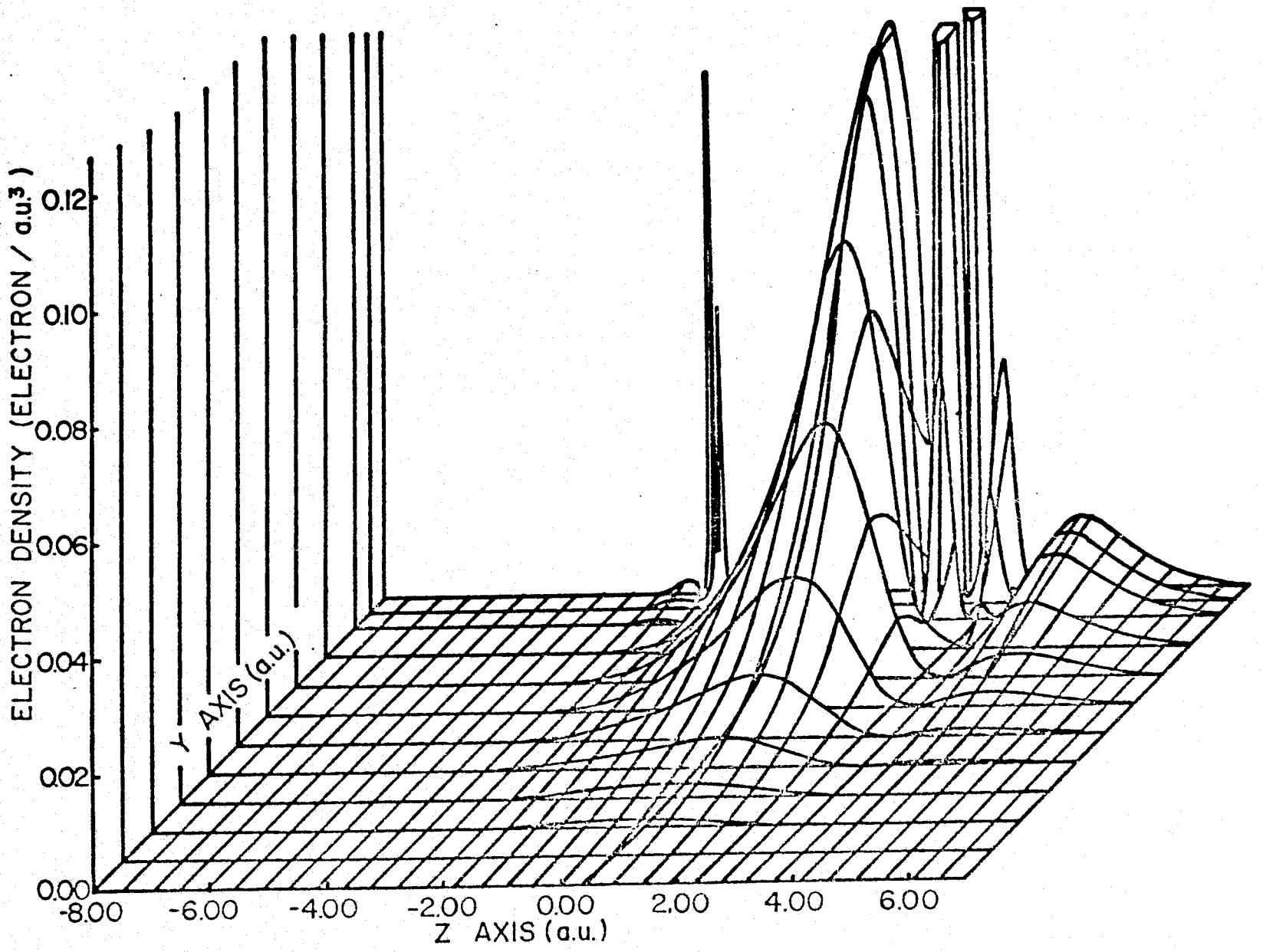
ELECTRON DENSITY (ELECTRON / a.u.^{3})
0.12
0.10
0.08
0.06
0.04
0.02
0.00
Y AXIS (a.u.)
-8.00
-6.00
-4.00
-2.00
0.00
2.00
4.00
6.00
Z AXIS (a.u.)

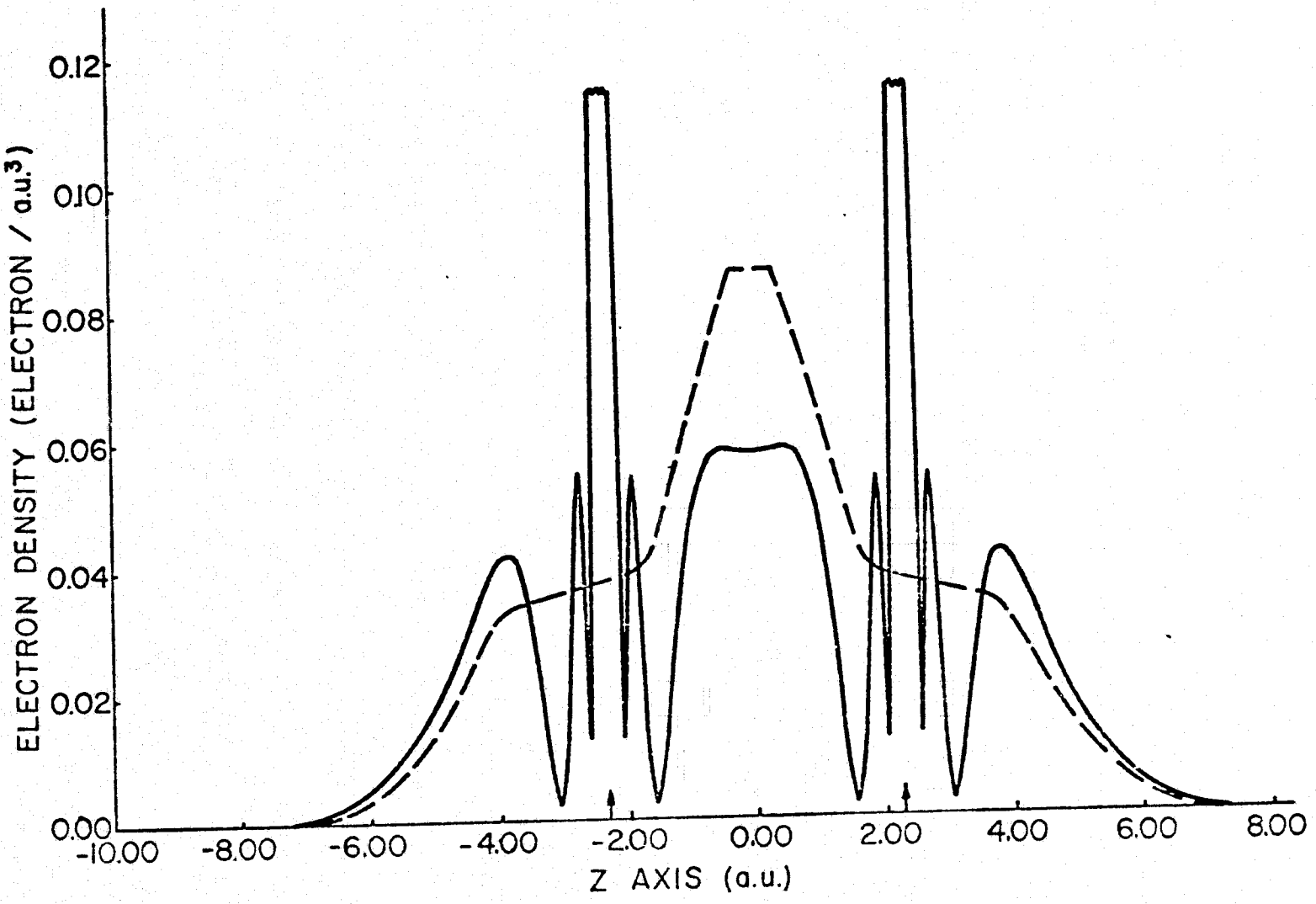
ELECTRON DENSITY (ELECTRON / a.u.^{3})
0.12
0.10
0.08
0.06
0.04
0.02
0.00
-10.00
-8.00
-6.00
-4.00
-2.00
0.00
2.00
4.00
6.00
8.00
Z AXIS (a.u.)

Fig. 5

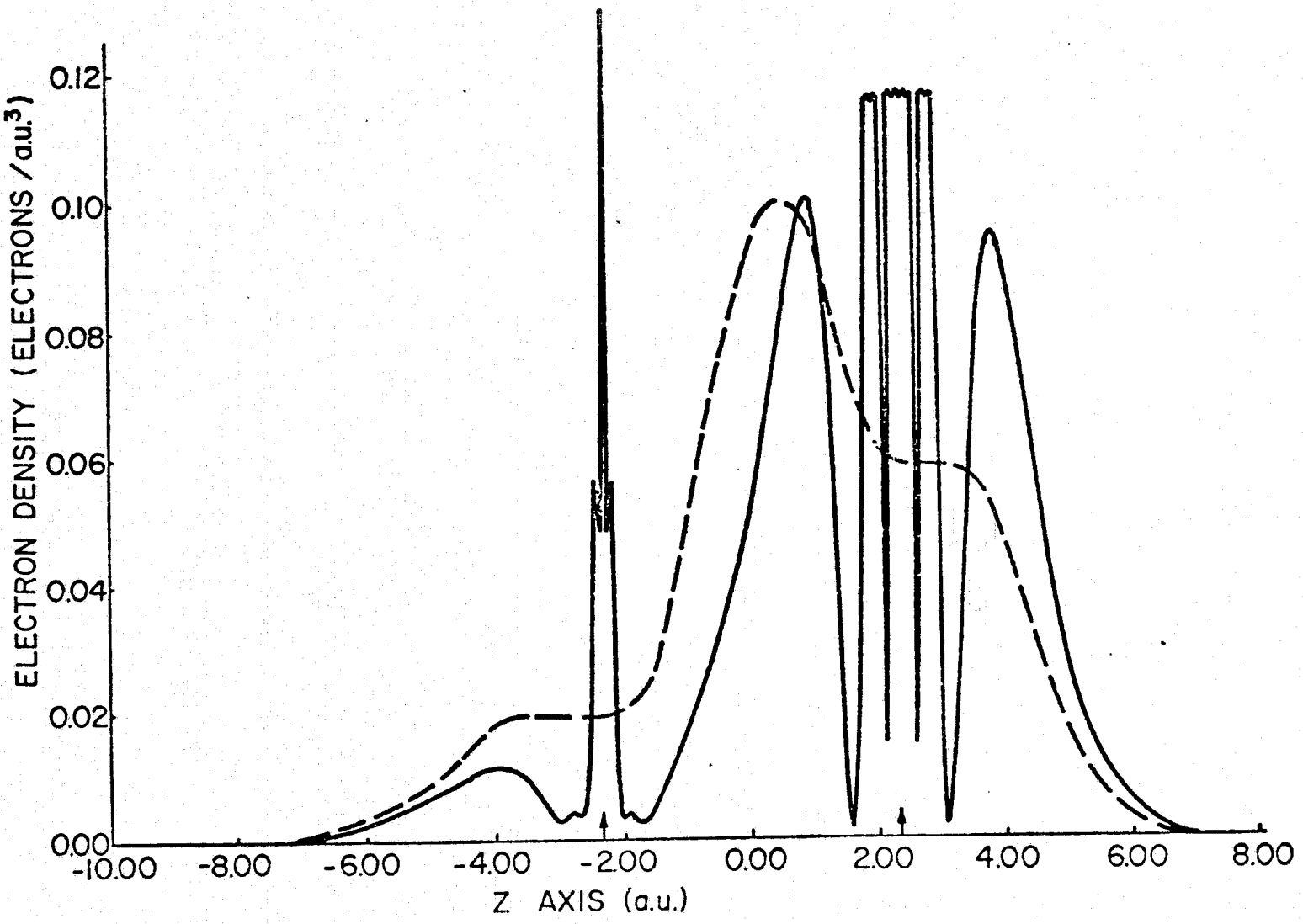
ELECTRON DENSITY (ELECTRONS /a.u.³)
0.12
0.10
0.08
0.06
0.04
0.02
0.00
-10.00
-8.00
-6.00
-4.00
-2.00
0.00
2.00
4.00
6.00
8.00
Z AXIS (a.u.)

Fig. 6

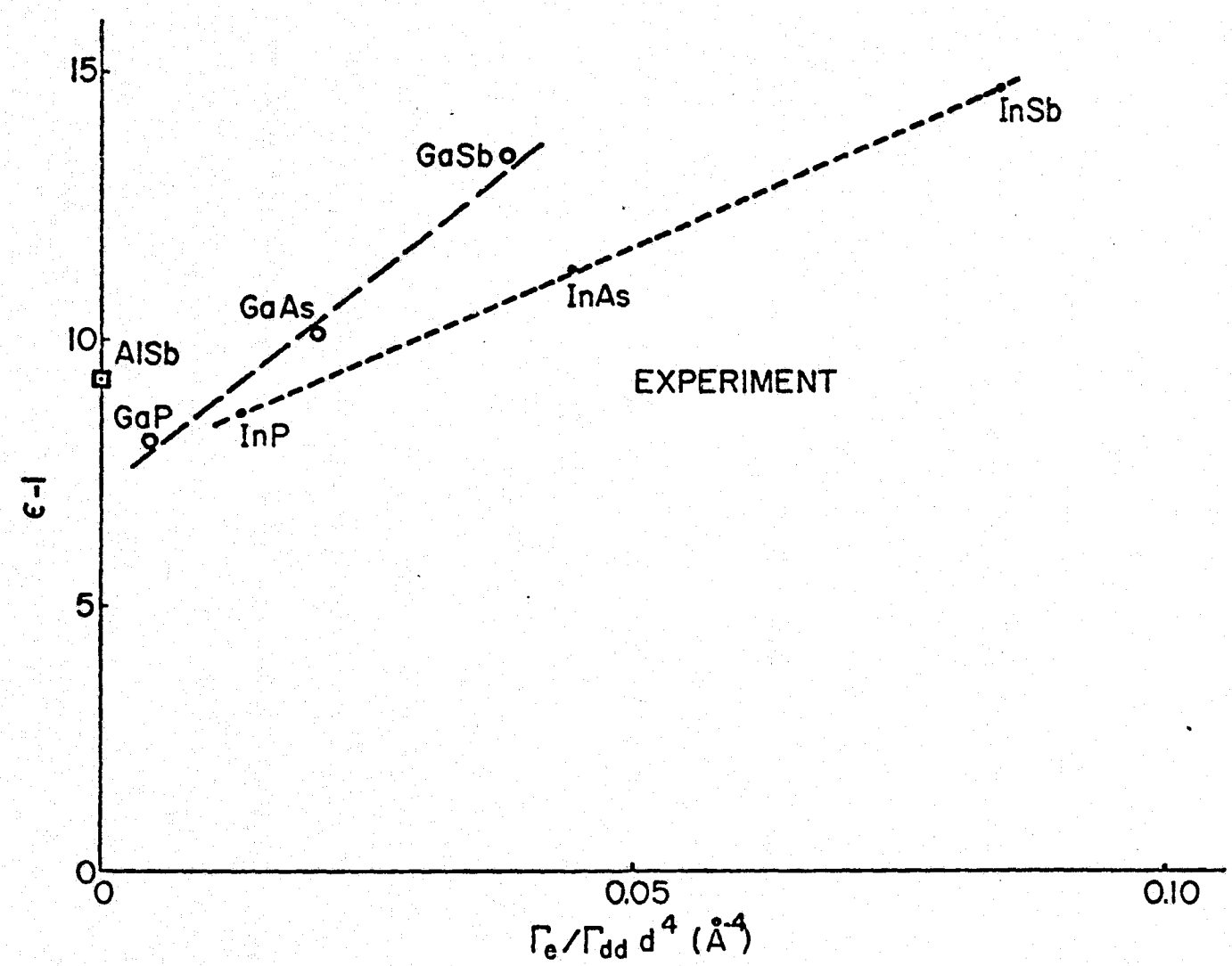
15
10
5
0
0
0.05
0.10
ε-1
AlSb
GaP
GaAs
GaSb
InP
InAs
InSb
EXPERIMENT
Γe/Γdd d4 (Å-4)

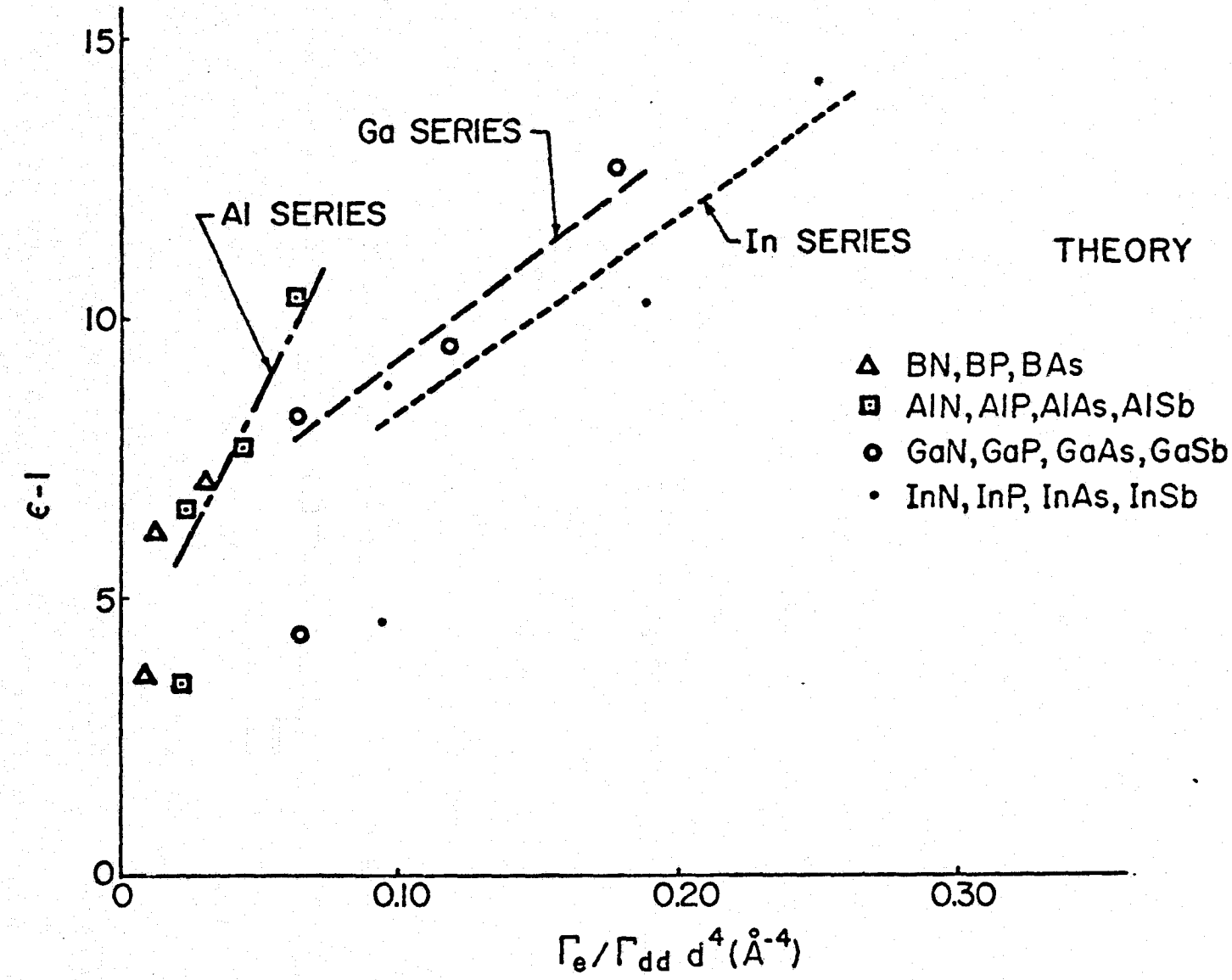
15
10
5
0
0
0.10
0.20
0.30
ε-1
$\Gamma_e/\Gamma_{dd}\, d^4$ (Å^{-4})
Ga SERIES
Al SERIES
In SERIES
THEORY
BN, BP, BAs
AlN, AlP, AlAs, AlSb
GaN, GaP, GaAs, GaSb
InN, InP, InAs, InSb

Fig. 8

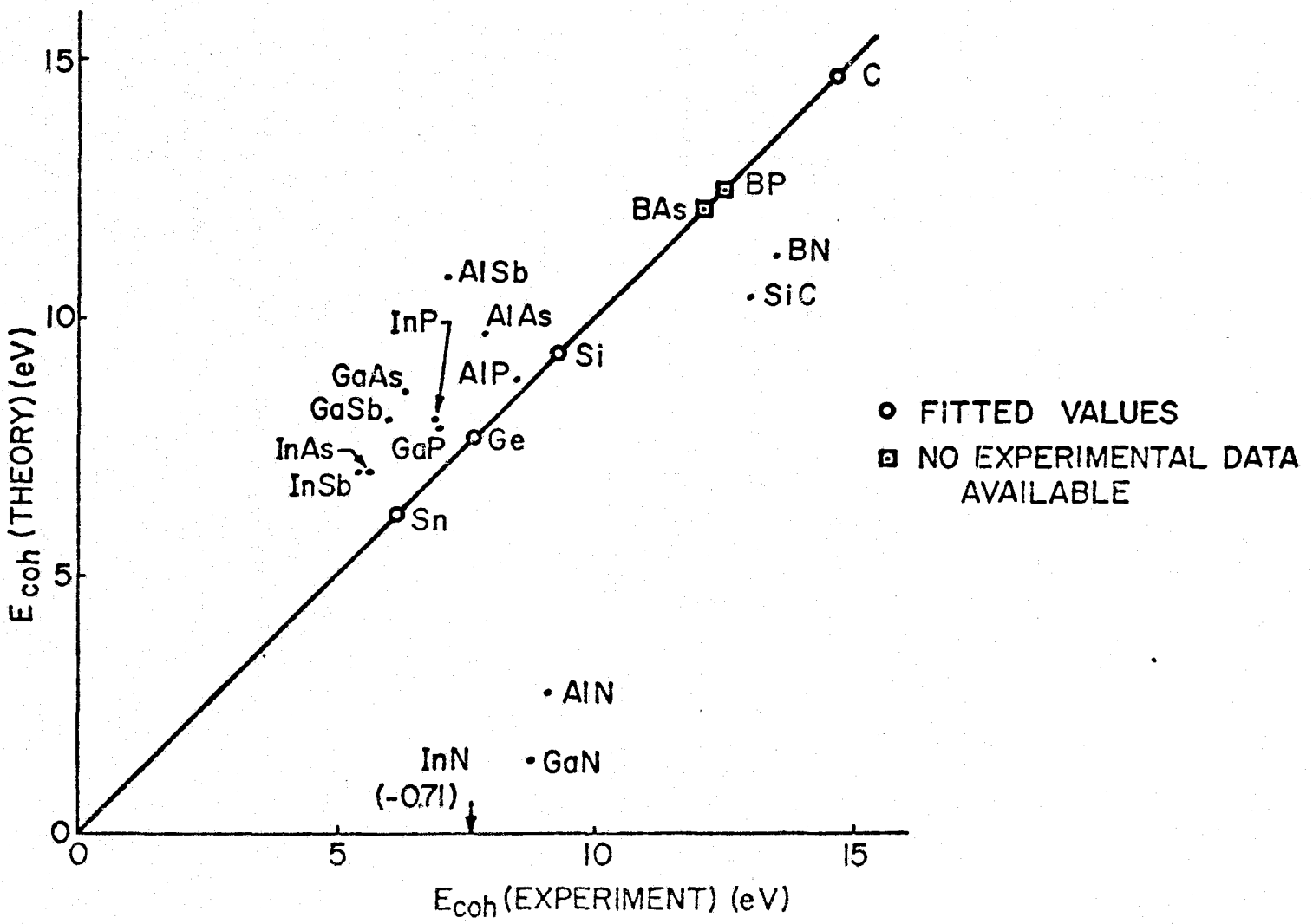
15
10
5
0
0
5
10
15
E_{coh} (THEORY) (eV)
E_{coh} (EXPERIMENT) (eV)
C
BP
BAs
BN
SiC
AlSb
InP
AlAs
Si
GaAs
AlP
GaSb
InAs
InSb
GaP
Ge
Sn
AlN
InN
(-0.71)
GaN
FITTED VALUES
NO EXPERIMENTAL DATA AVAILABLE